Statistical properties of polarized dust emission : lessons from a toy model of the turbulent and magnetized interstellar medium

François Levrier

LERMA, Observatoire de Paris, PSL, CNRS, UPMC, ENS Paris

Thanks to Jérémy Neveu

l'Observatoire de Paris | LERMA

Laboratoire d'Étude du Rayonnement et de la Matière en Astrophysique

Magnetic Fields in the Universe V, Cargèse, 5-9 October 2015

The Planck view of the Galactic magnetic field

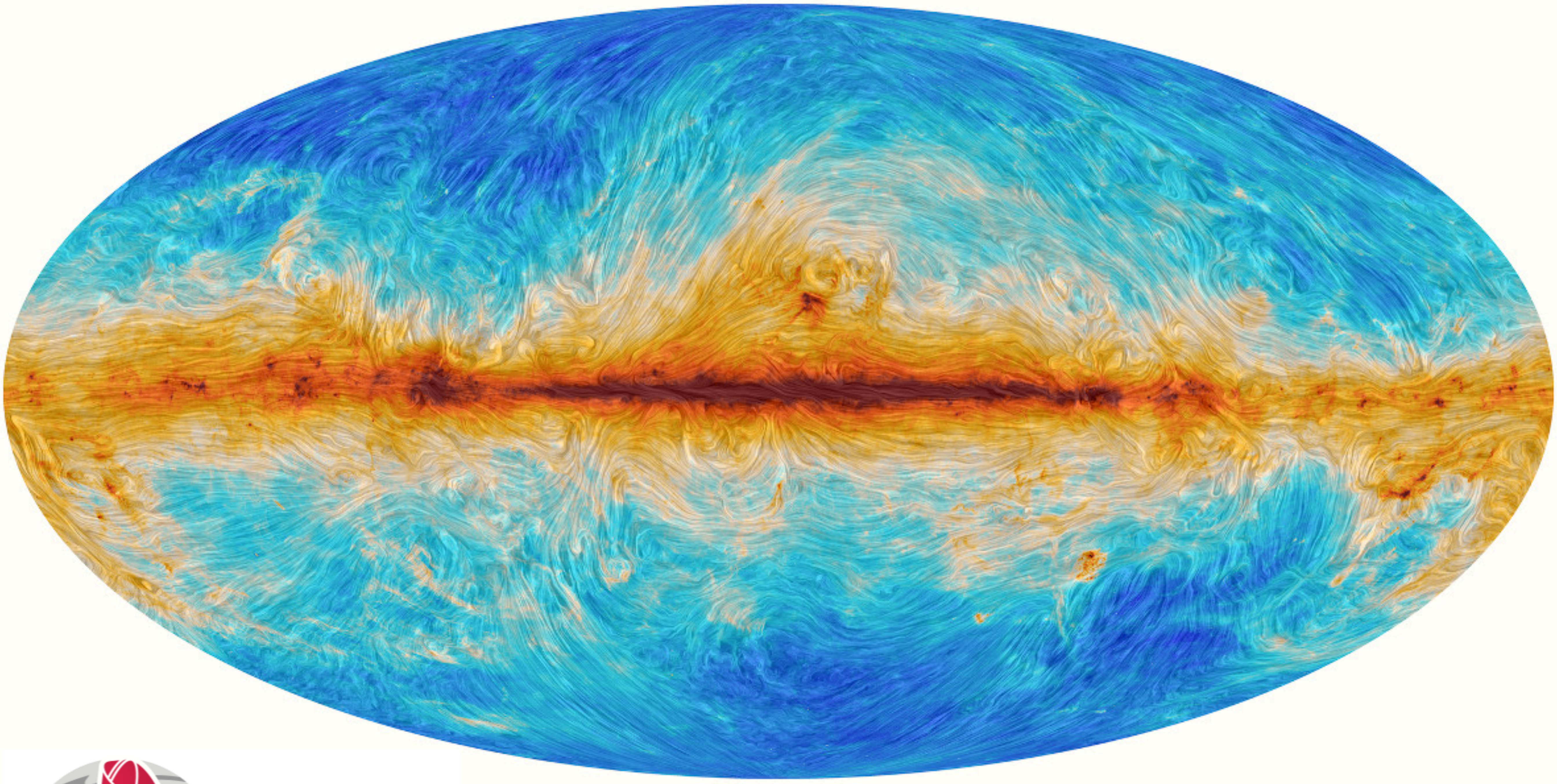

planck

Planck intermediate results XIX, XX, XXI, XXII, XXX, XXXII, XXXIII, XXXIV, XXXV, XXXVIII

Polarized emission towards Ophiuchus

Polarization fraction

$$p = \frac{\sqrt{Q^2 + U^2}}{I}$$

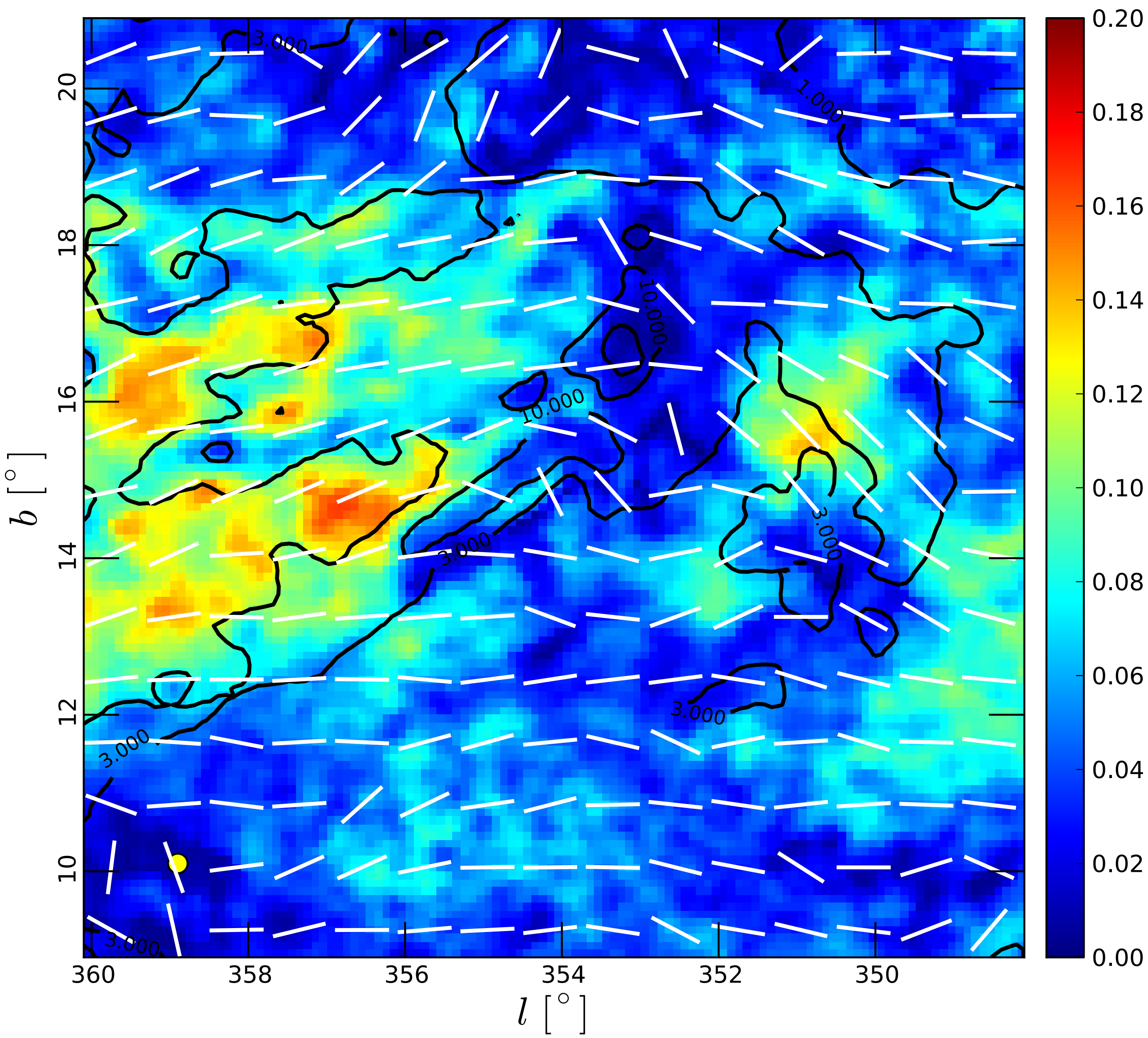

Polarization angle dispersion function

$$\mathcal{S}(\boldsymbol{r}, \delta) = \sqrt{\frac{1}{N} \sum_{i=1}^{N} \left[\psi(\boldsymbol{r} + \boldsymbol{\delta}_i) - \psi(\boldsymbol{r})\right]^2}$$

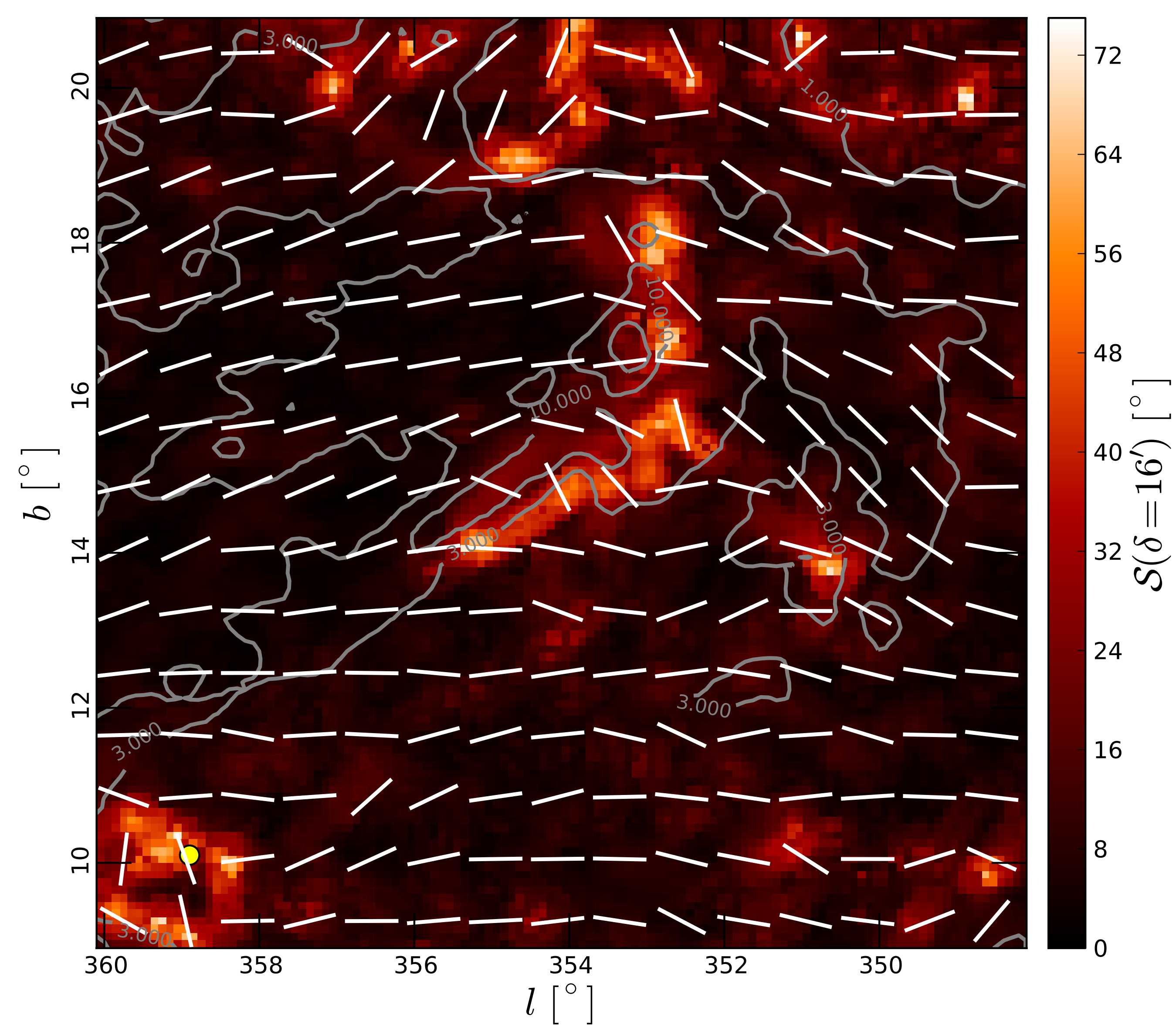

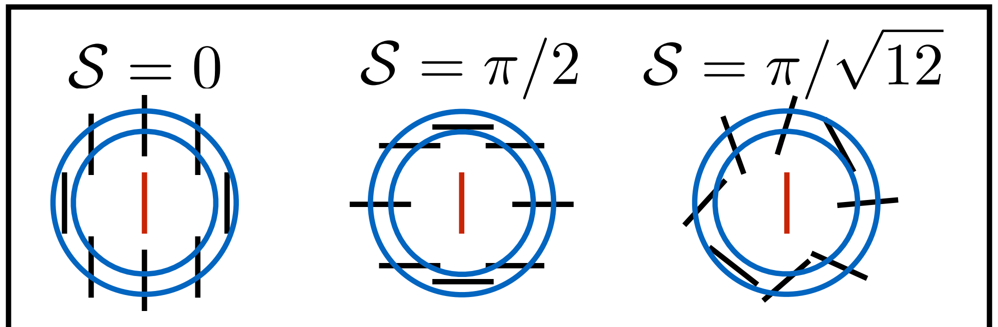

15' resolution
16' lag δ

Polarization fraction vs. column density

$p/\sigma_p > 3$

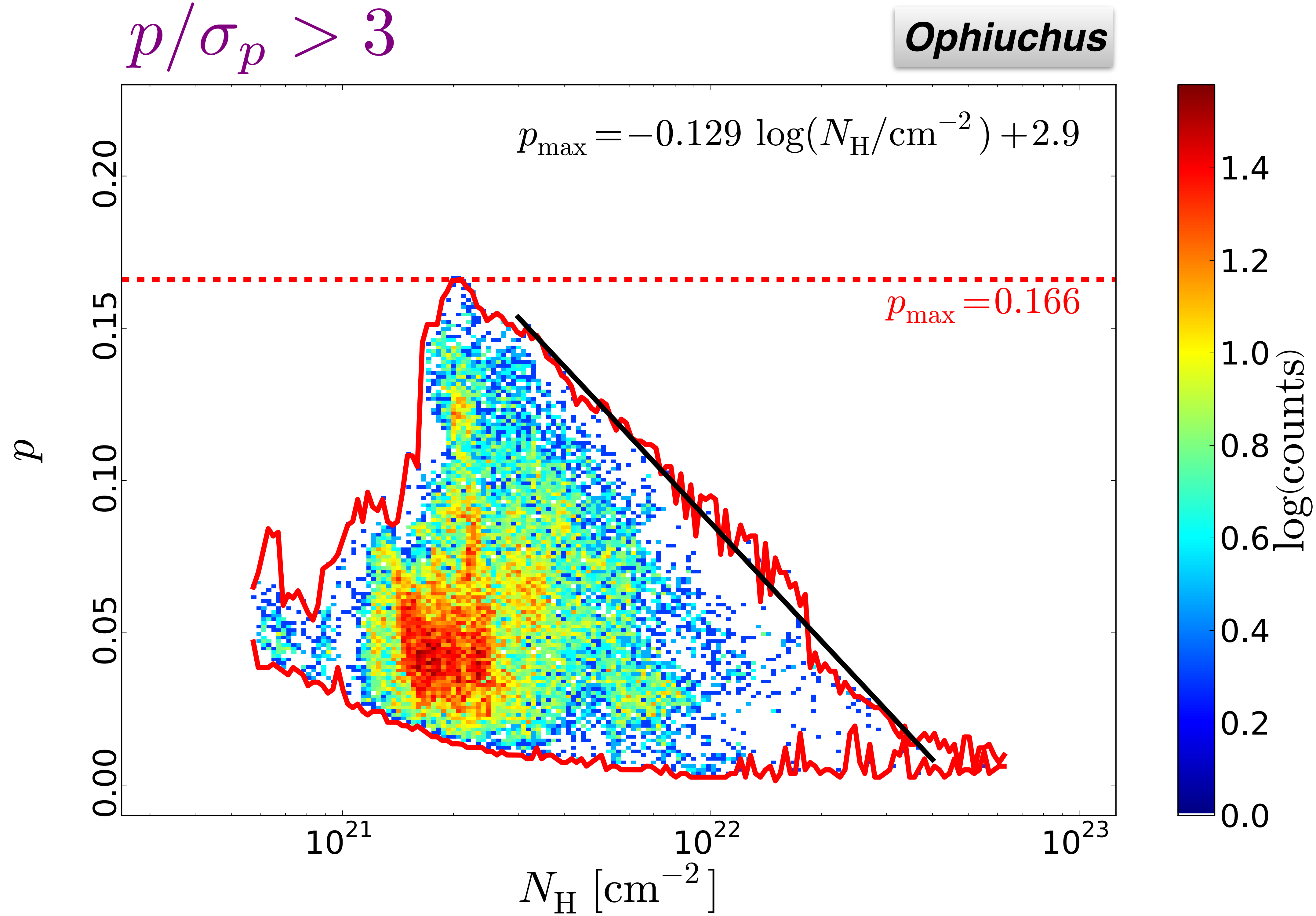

Anti-correlation robust with respect to polarization S/N

Angular dispersion vs. polarization fraction

Ophiuchus

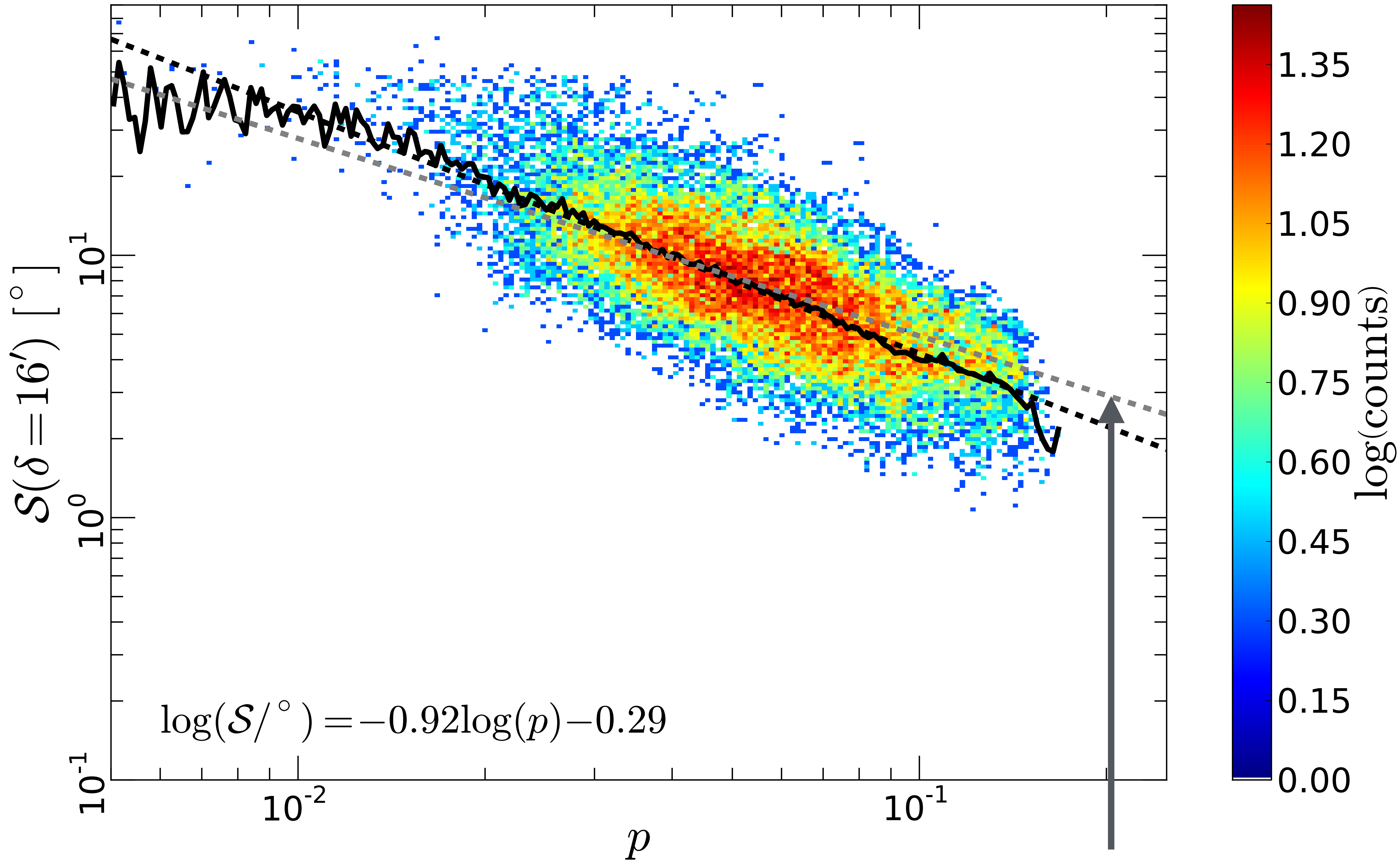

« All-sky » fit

Planck intermediate results. XIX. A&A, 576, 104, 2015

Building simulated polarized emission maps

- Ideal MHD with self-gravity
- An 18 pc subset of a 50 pc simulation cube
- Converging flows of magnetized warm gas
- Mean magnetic field along the flows
- Rotation of the cube, placed at 100 pc
- Simulated Stokes maps at 353 GHz smoothed at 15'

Top-down view

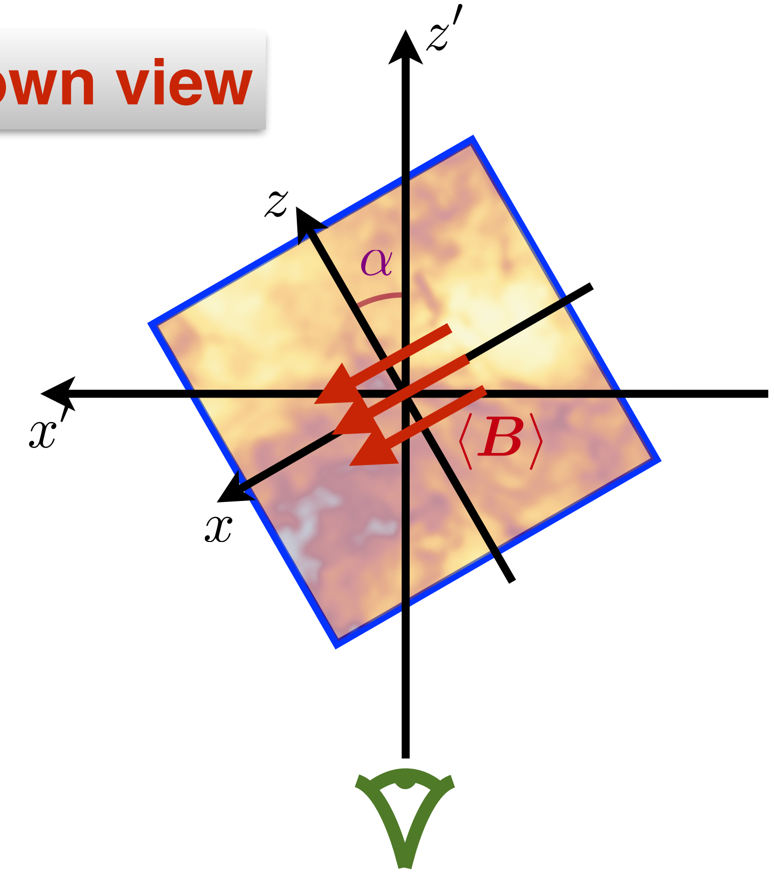

$$I = \int S_\nu e^{-\tau_\nu} \left[1 - p_0 \left(\cos^2\gamma - \frac{2}{3}\right)\right] \mathrm{d}\tau_\nu$$

$$Q = \int p_0 S_\nu e^{-\tau_\nu} \cos(2\phi) \cos^2\gamma \mathrm{d}\tau_\nu$$

$$U = \int p_0 S_\nu e^{-\tau_\nu} \sin(2\phi) \cos^2\gamma \mathrm{d}\tau_\nu$$

« Intrinsic dust polarization parameter »

$$p_0 = 0.2$$

Opacity at 353 GHz (Planck Collaboration XXXI, 2014)

$$\tau_{353}/N_{\mathrm{H}} = 1.2 \times 10^{-26}\,\mathrm{cm}^2$$

Dust temperature

$$T_d = 18\,\mathrm{K}$$

Side view

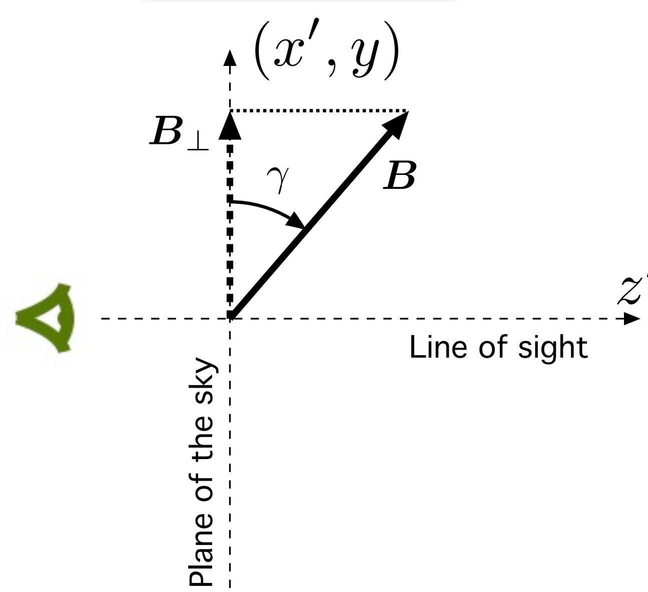

Line-of-sight view

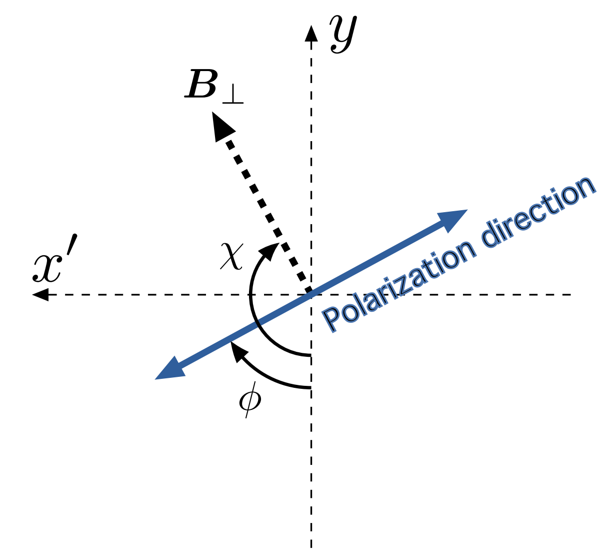

See also Diego Falceta-Gonçalves' talk

Hennebelle et al. 2008

starformat.obspm.fr

Simulations vs. Observations

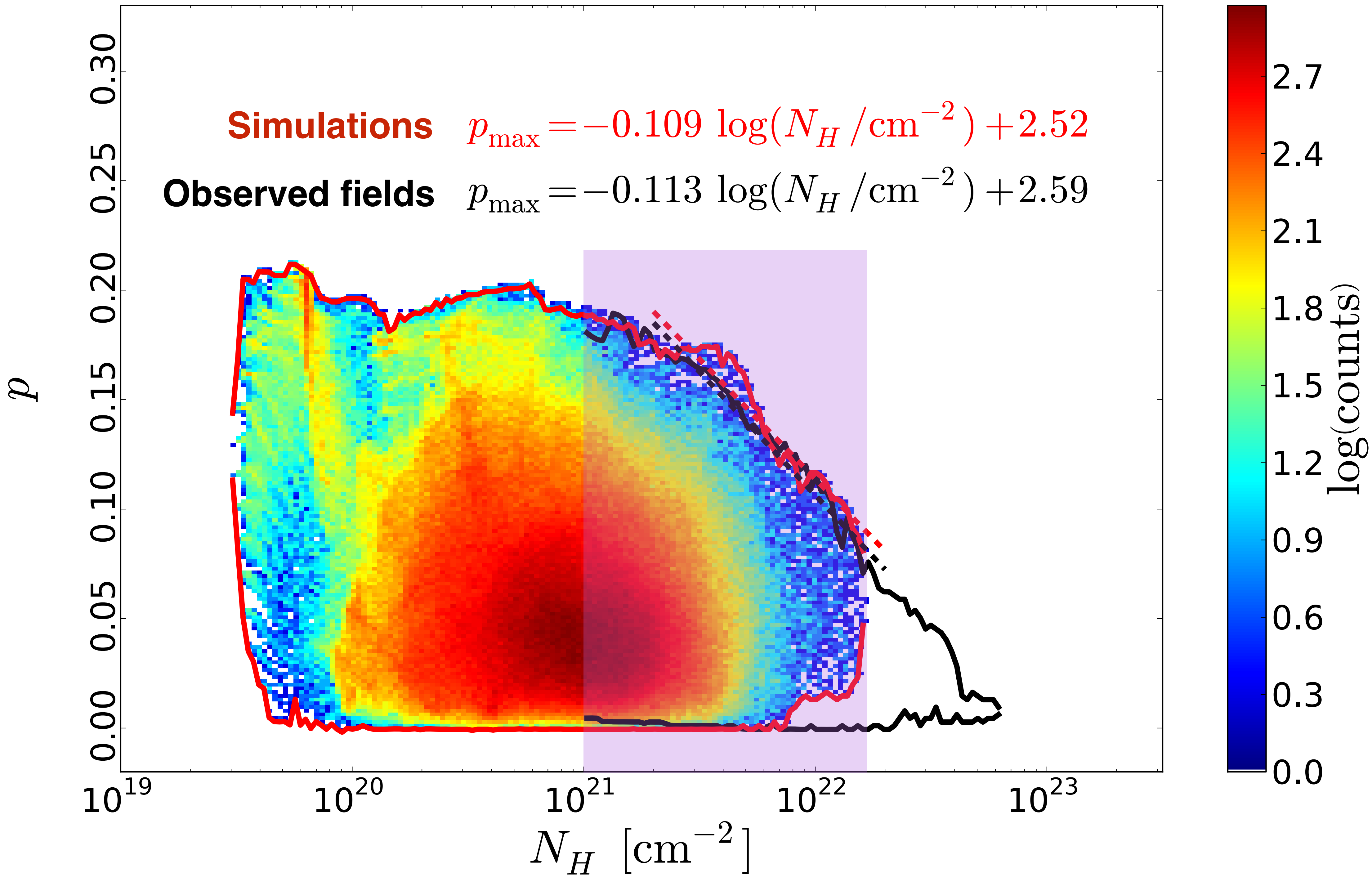

Simulations reproduce very well the decrease of $p_{\max}$ with $N_{\rm H}$ in the range 10^{21} to 2×10^{22} cm^{-2}

See also Diego Falceta-Gonçalves' talk

Simulations vs. Observations

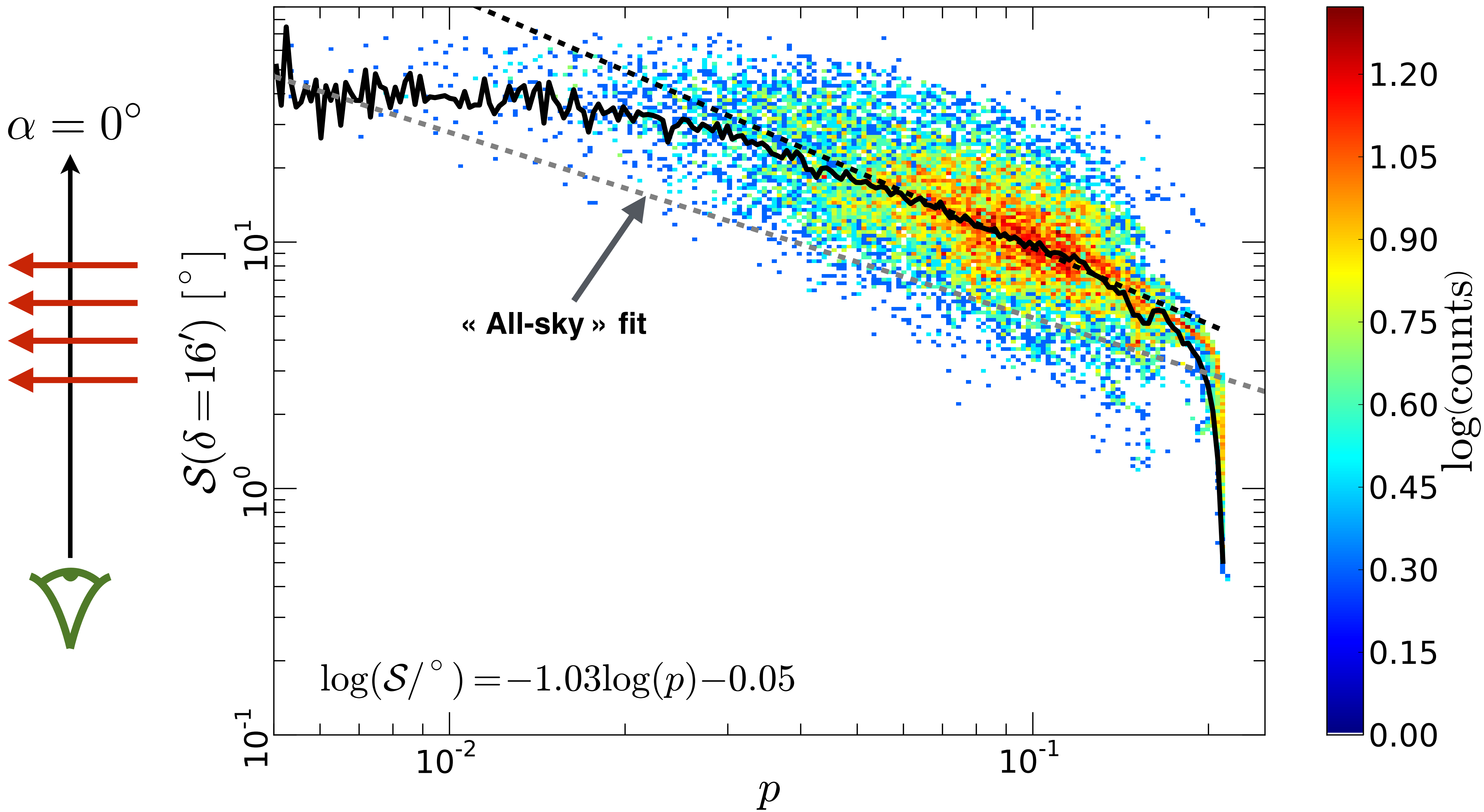

Global trend is reproduced, but simulations tend to have too high an angular dispersion

From reality to observables and back again ?

We wish to constrain the statistical properties of the interstellar B field

Physical fields → **Observables**

$n, T, \vec{B}, \vec{v}, \ldots$

$I, Q, U, p, \psi, \mathcal{S}, \ldots$

- ***Density spectral index*** β_n
- ***B spectral index*** β_B
- ***Density fluctuation level*** $\sigma_n / \langle n \rangle$
- ***B fluctuation level*** $\sigma_B / \langle B \rangle$
- ***Line-of-sight depth*** d

$\ldots$

PDFs

Power spectra

Correlations

...

Building a toy dust density field

log-density built as a fractional Brownian motion (fBm)

inverse FT

$$\tilde{X}\left(\boldsymbol{k}\right) = A_0 |\boldsymbol{k}|^{-\beta} \exp\left[i\phi(\boldsymbol{k})\right]$$

$$n\left(\boldsymbol{r}\right) = n_0 \exp\left[\frac{X\left(\boldsymbol{r}\right)}{X_0}\right]$$

- **Power-law amplitudes**
- **Random phases**

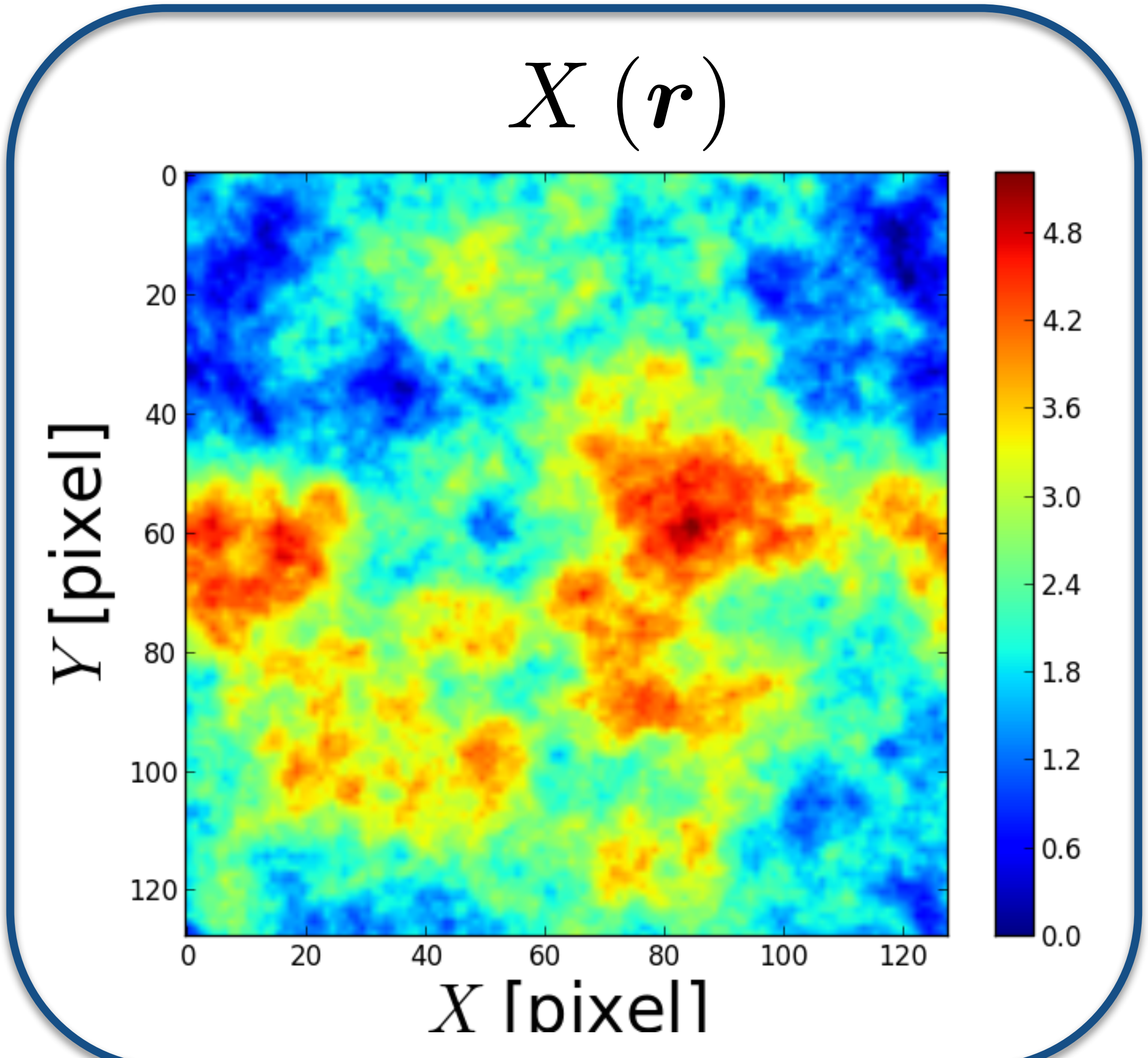

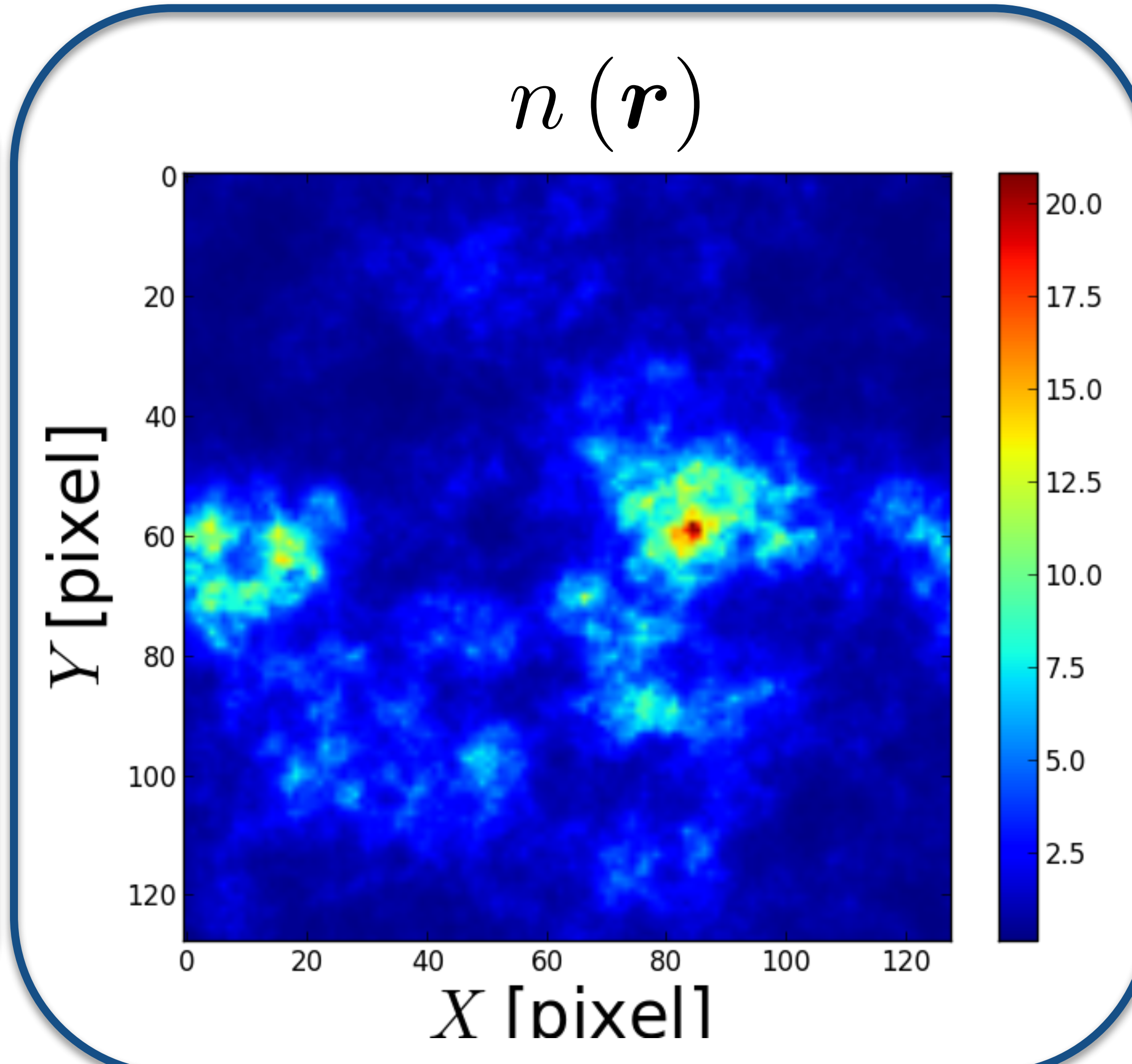

Properties of the toy dust density field

$$n(\boldsymbol{r}) = n_0 \exp\left[\frac{X(\boldsymbol{r})}{X_0}\right]$$

- **Power-law power spectrum**
- **Spectral index close to that of the log-density**

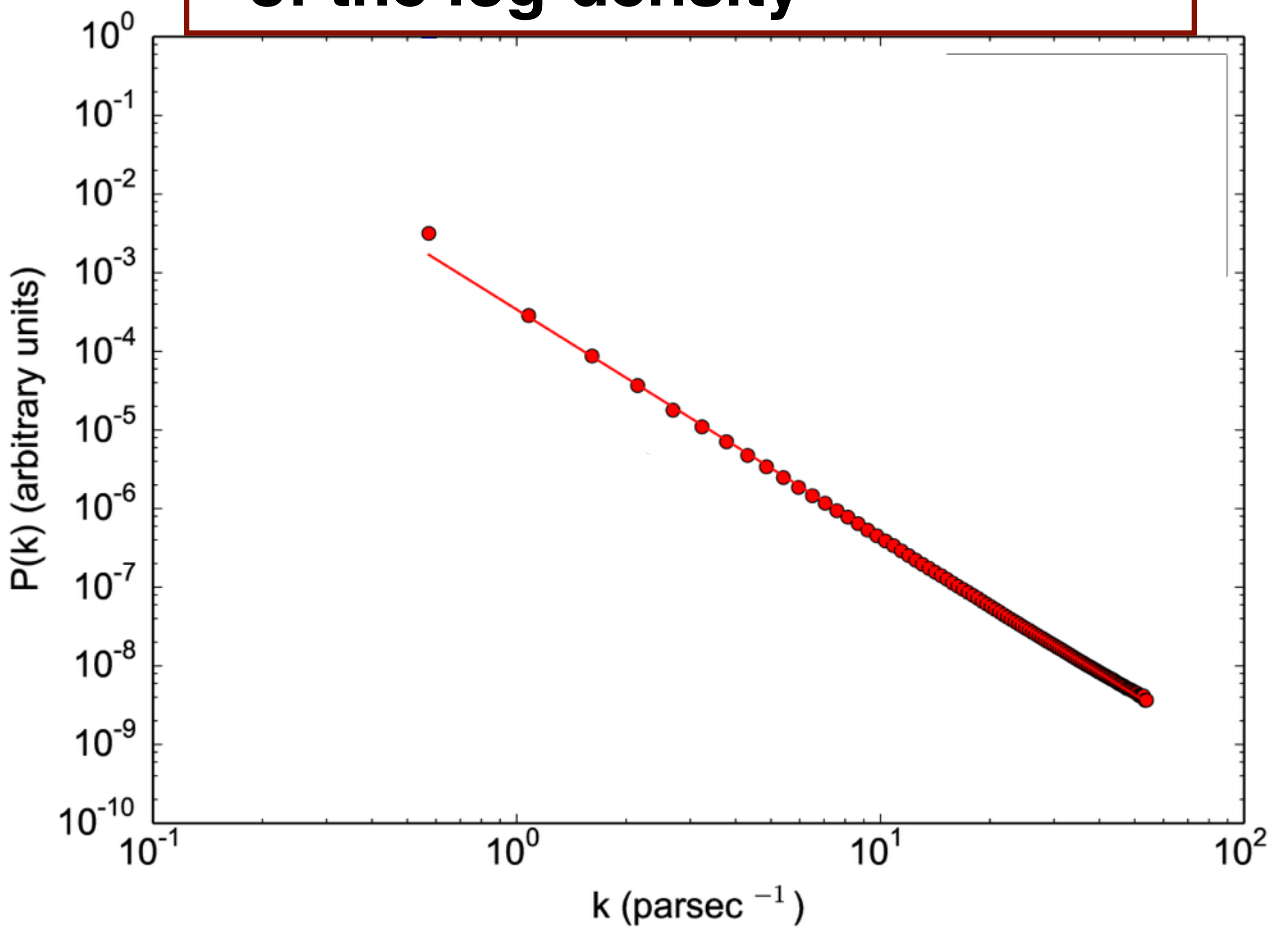

- **Close to log-normal PDF**
- **Possibly large fluctuations**

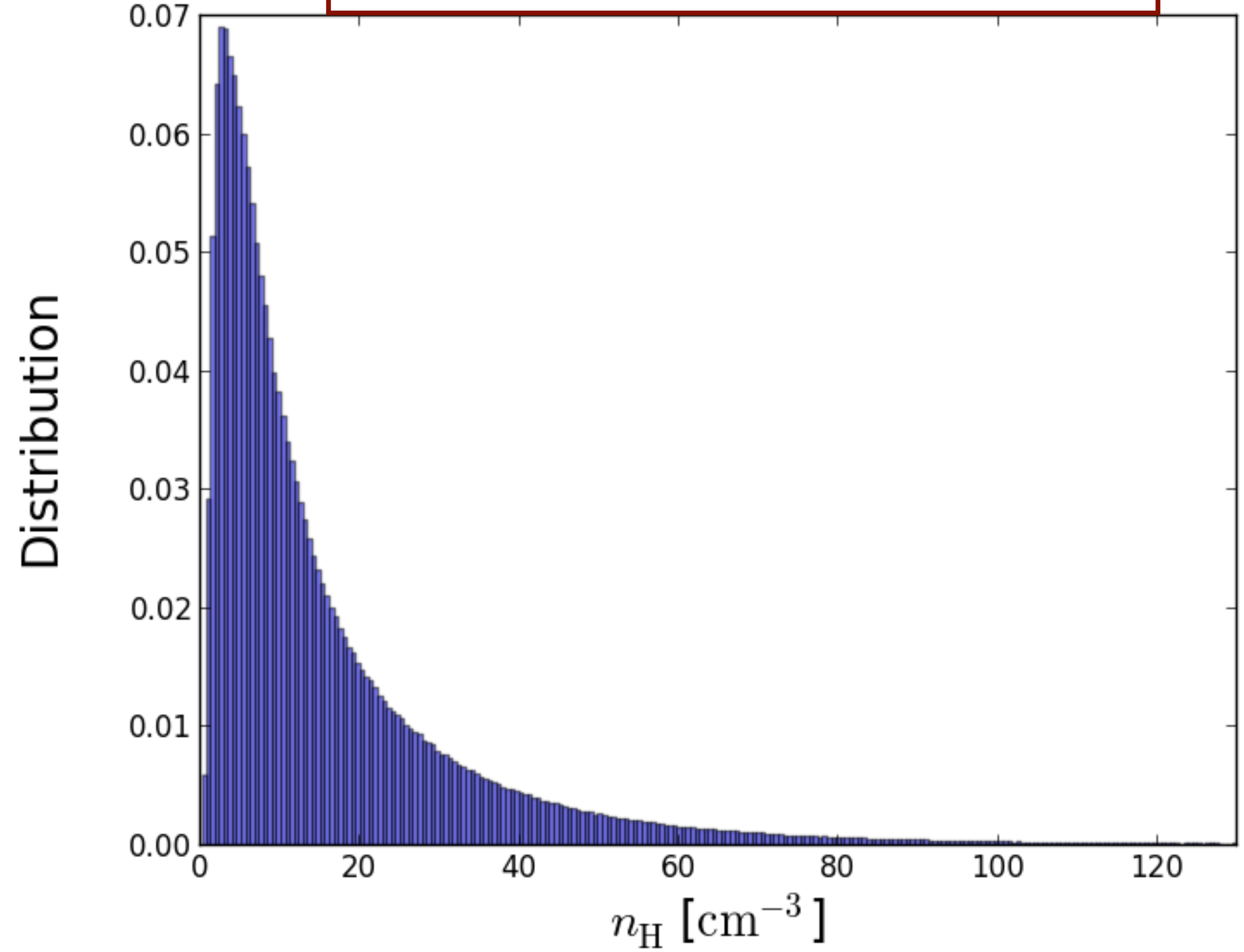

NB : for fBm fields $\frac{\sigma_X}{\langle X \rangle} < 0.3$

Building a toy magnetic field

Magnetic field built from fBm vector potential components

$$\boldsymbol{B} = \boldsymbol{\nabla} \times \boldsymbol{A}$$

$\widetilde{A_\nu}(\boldsymbol{k})$ **fBm fields**

$$\widetilde{B_\lambda}(\boldsymbol{k}) = \epsilon_{\lambda\mu\nu} i k_\mu \mathcal{F}_0 |\boldsymbol{k}|^{-\beta_A/2} \exp\left[i\phi_{A_\nu}(\boldsymbol{k})\right]$$

Levi-Civita tensor

Input spectral index

Input Fourier phase map

Component of the B field in Fourier space

inverse FT

$$B_\lambda(\boldsymbol{r})$$

Properties of the toy magnetic field

- Divergence-free
- Power-law power spectrum
- Gaussian PDF with zero mean
- Possibility to add a large-scale uniform field

$$\beta_B = \beta_A - 2$$

Probability distribution functions

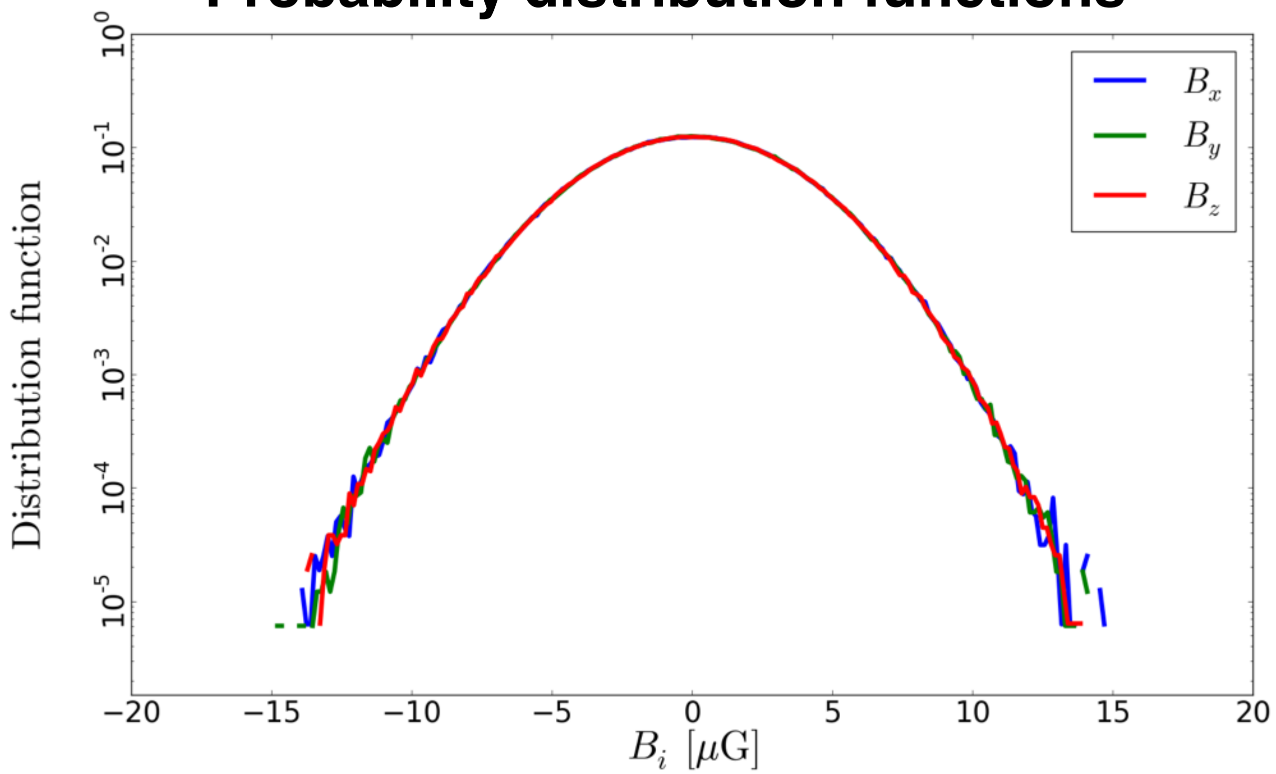

Power spectra

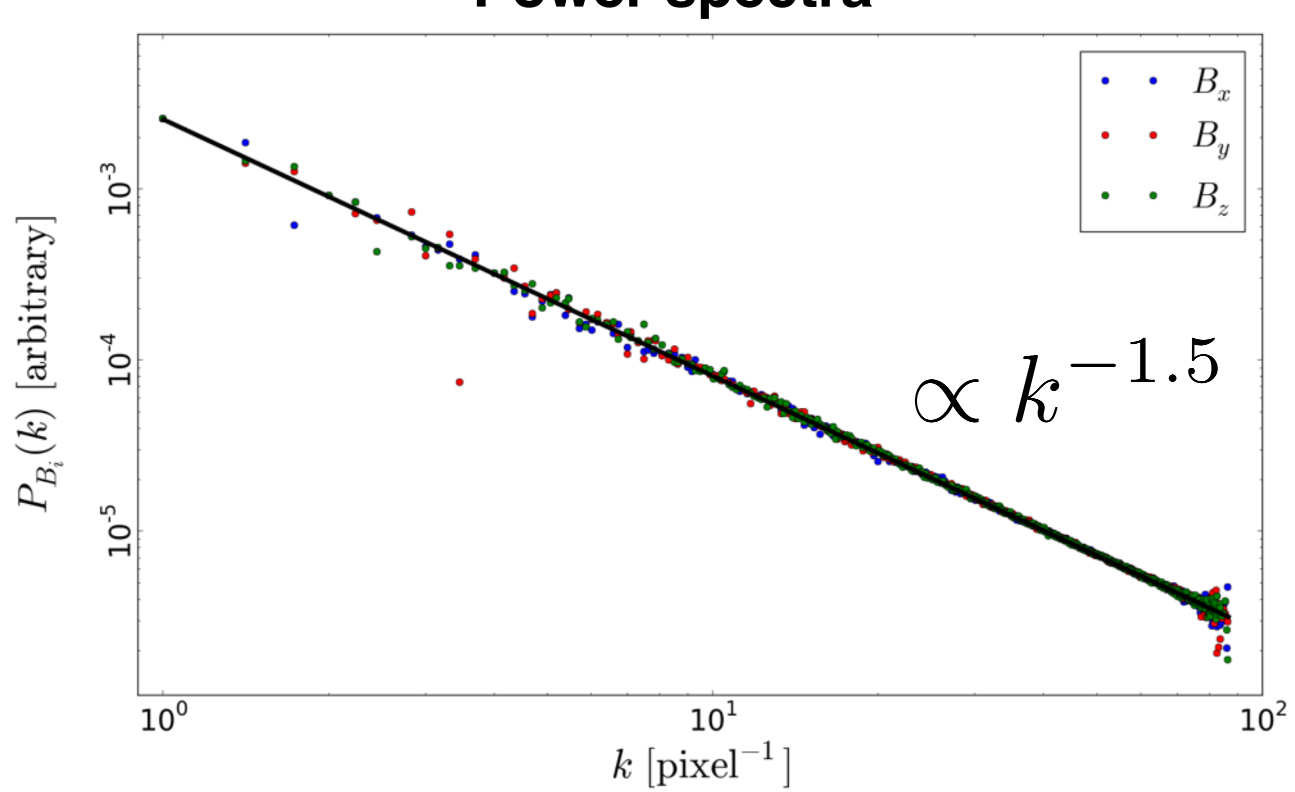

Physical parameters and observables

Physical parameters of the input cubes

- **Spectral indices**
- **Fluctuation ratios**
- **Depth**

$$\beta_n,\ \beta_B,\ \frac{\sigma_n}{\langle n_{\rm d}\rangle},\ \frac{\sigma_B}{\langle B\rangle},\ d$$

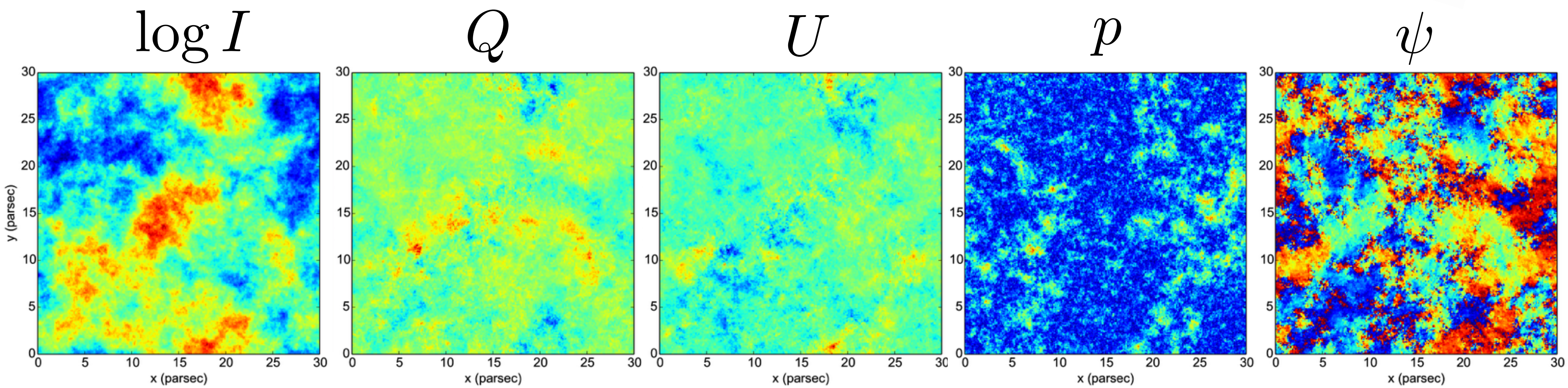

...

Observables derived from simulated Stokes maps

- **Spectral indices of** $I,\ Q,\ U,\ P$
- **Fluctuation ratios of** $I,\ P$
- **Position of PDF maximum of** $\mathcal{S},\ p,\ |\nabla P|/P$
- **Correlation** $\mathcal{S}\ \mathrm{vs.}\ p$
- **Correlation** $\mathcal{S}\ \mathrm{vs.}\ |\nabla P|/P$

Validating the method

A least-square analysis validates the method on simulated maps

$\beta_n = 3.2$

$\beta_B = 1.6$

$\frac{\sigma_n}{\langle n \rangle} = 1$

$\frac{\sigma_B}{\langle B \rangle} = 1$

$d = 40$

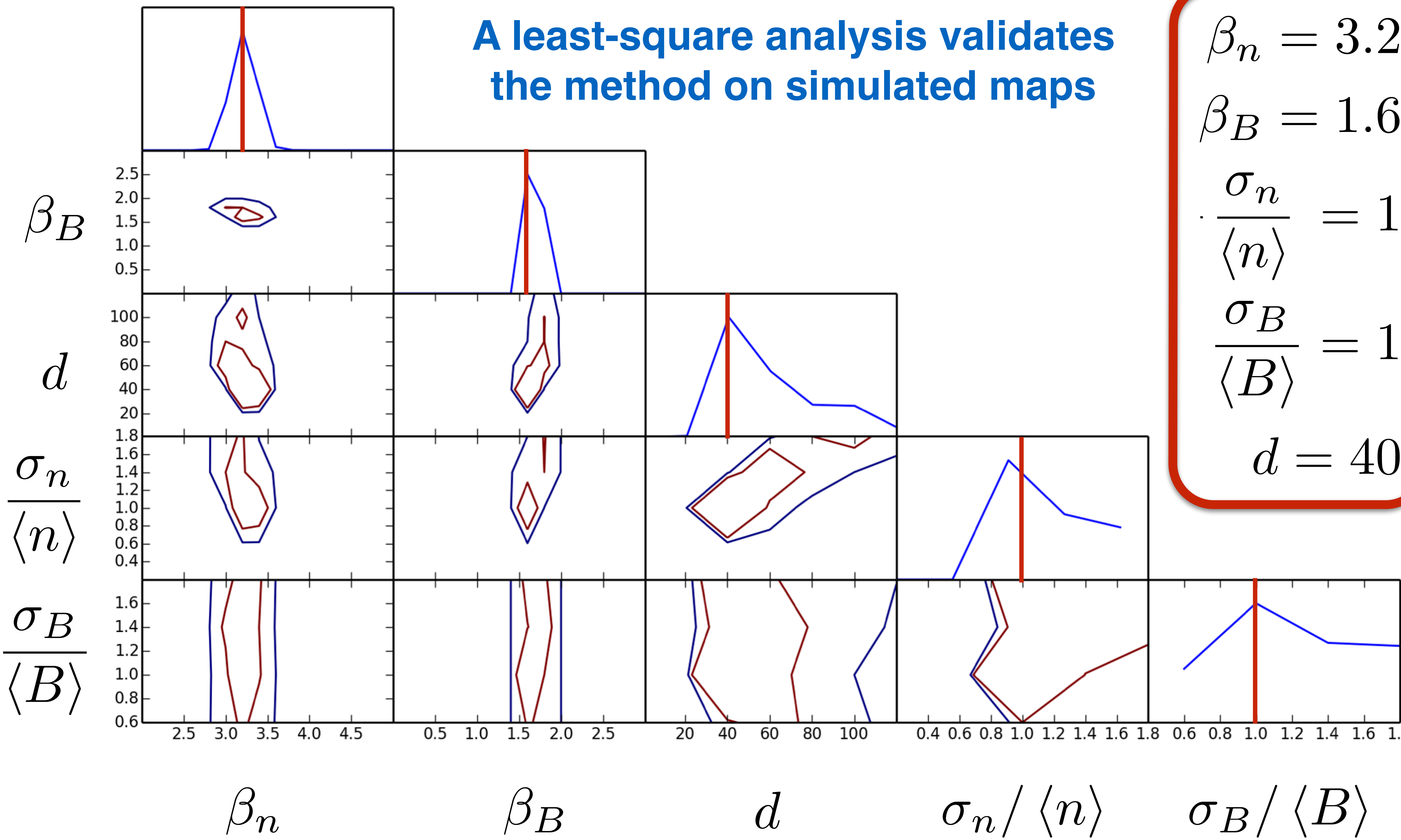

Application to Planck data

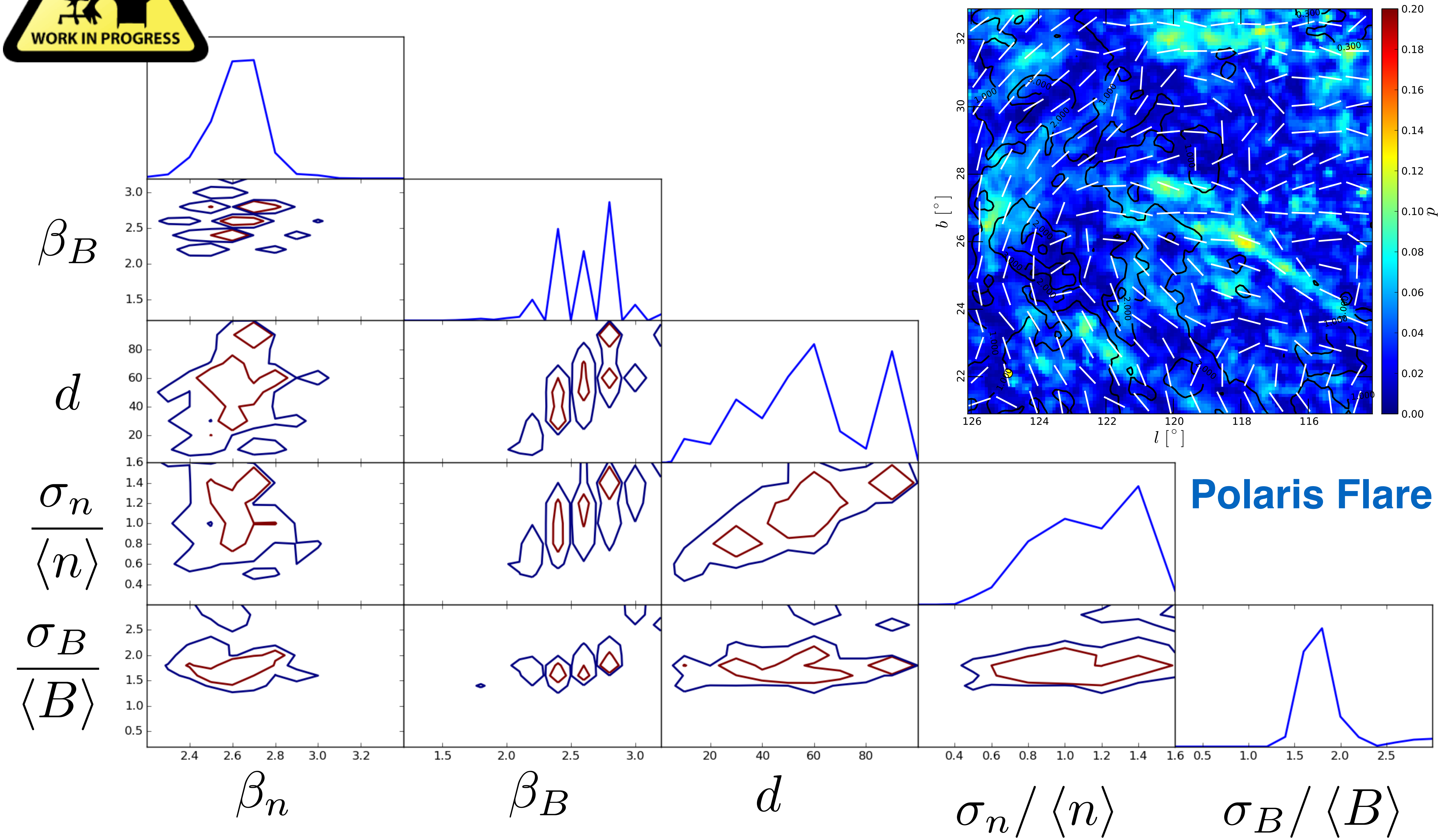

- **B spectral index near 2.6, consistent with approaches of Bracco and Vansyngel**
- **Power spectrum tends to steepen with increasing depth**

Conclusions

Comparison of Planck polarization maps with MHD simulations

- Decrease of p_{max} with N_H well reproduced by simulations
- Anticorrelation between polarization fraction and angle dispersion underlines the role of the magnetic field

Likelihood analysis to constrain statistical properties of ISM B

- Simple, controlled statistics, allowing thorough parameter space exploration
- Points to a magnetic spectral index near 2.6 in the Polaris Flare
- Consistent with an approach using dust polarization C_ℓ and a model with a finite number of layers (Boulanger, Bracco, Vansyngel))

Additional slides

Polarization fractions vs. column density

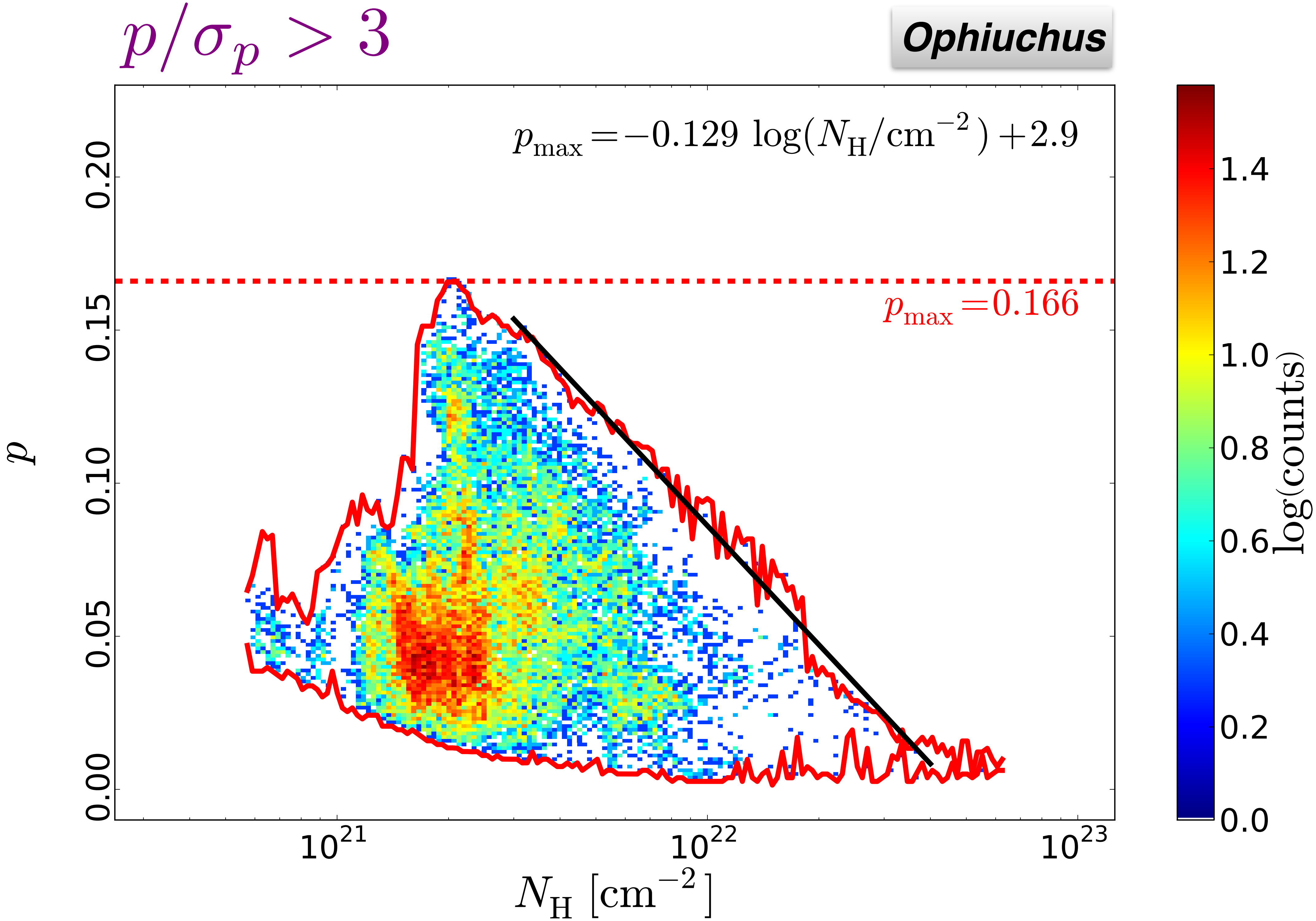

Anti-correlation robust with respect to polarization S/N

Polarization fractions vs. column density

$p/\sigma_p > 10$

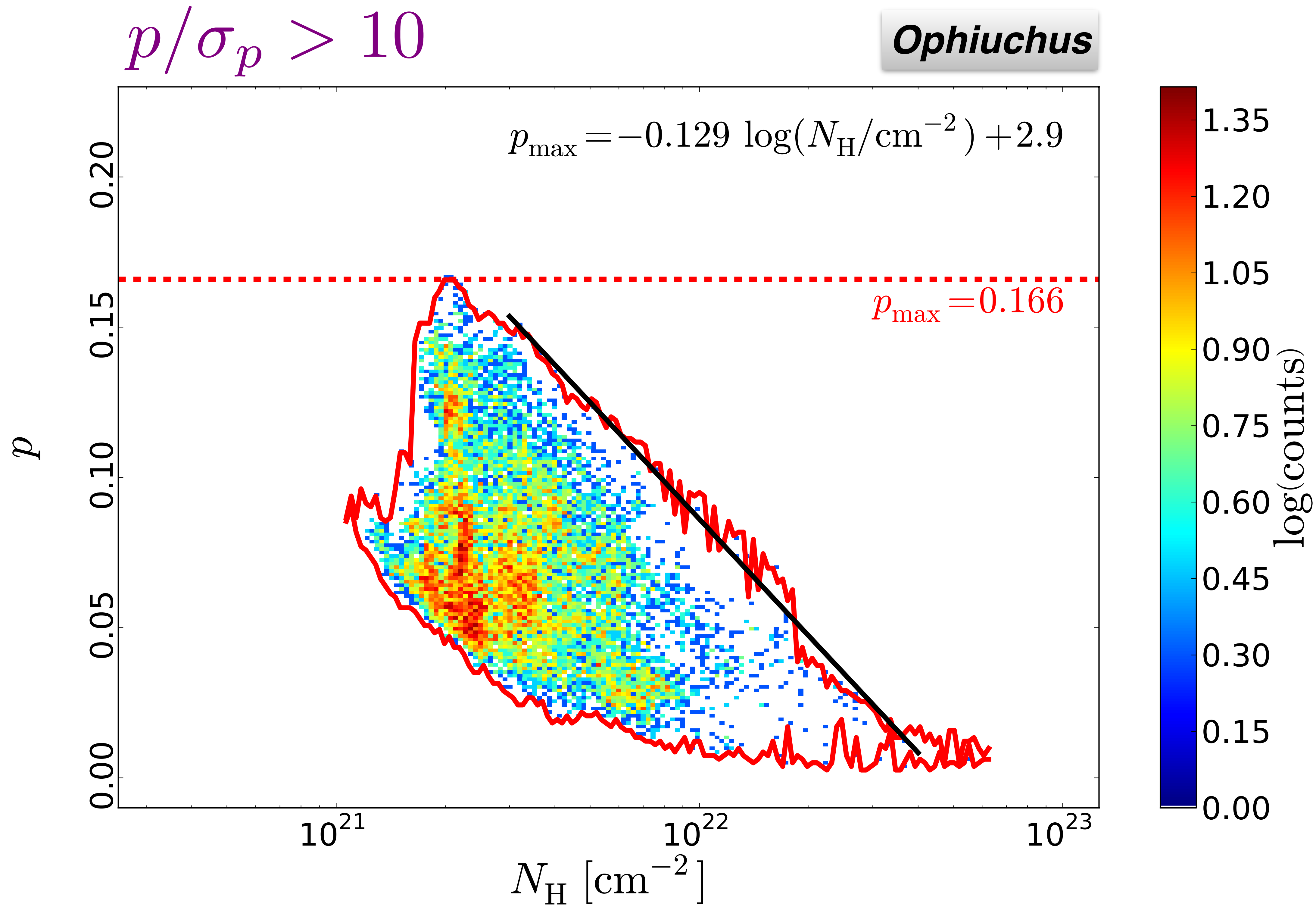

Anti-correlation robust with respect to polarization S/N

Simulated polarized thermal dust emission maps

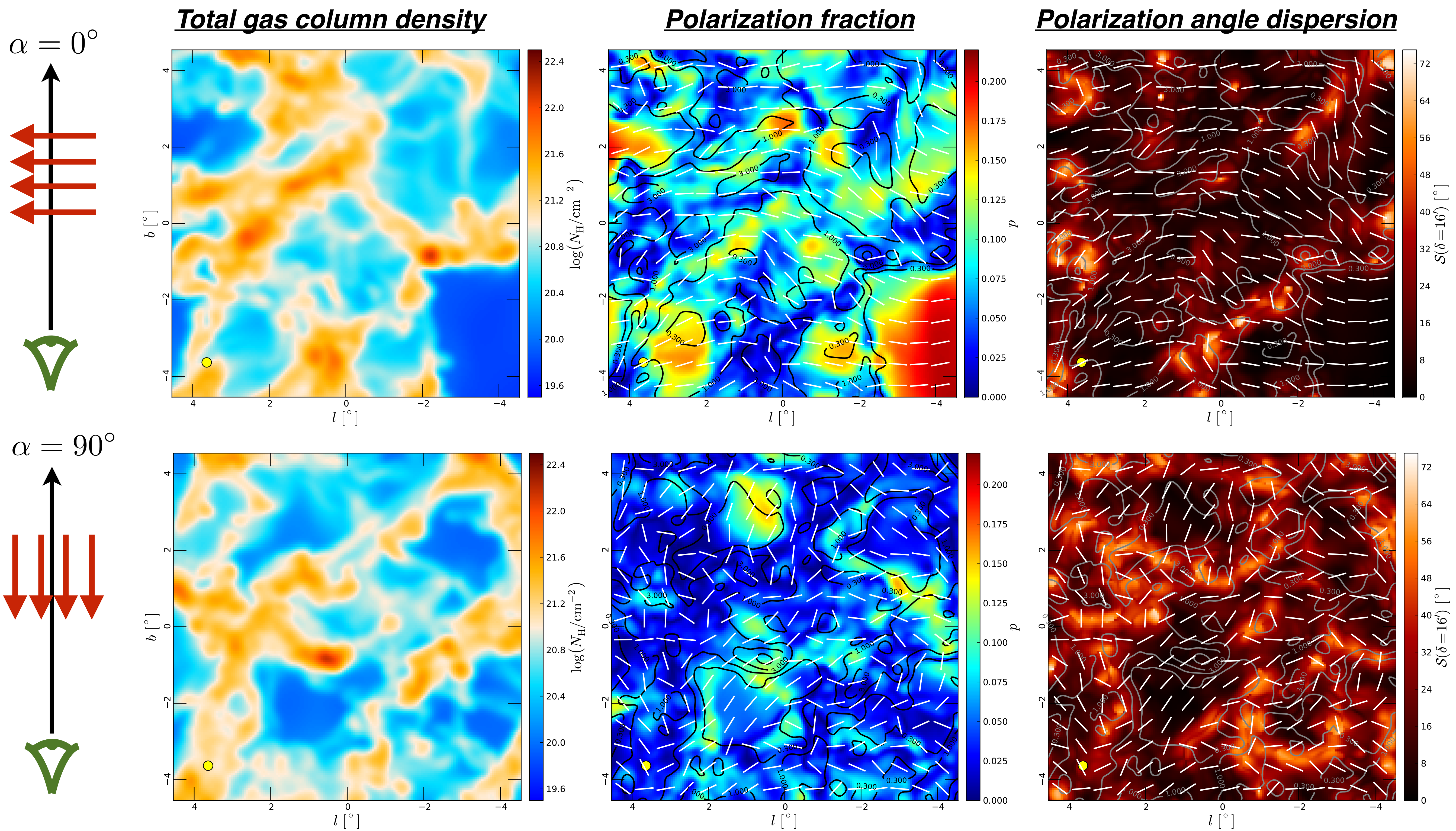

Anti-correlation p and $N_{\rm H}$

Anti-correlation p and $\mathcal{S}$

Lower polarization fractions when along the mean field

MHD simulation density PDF

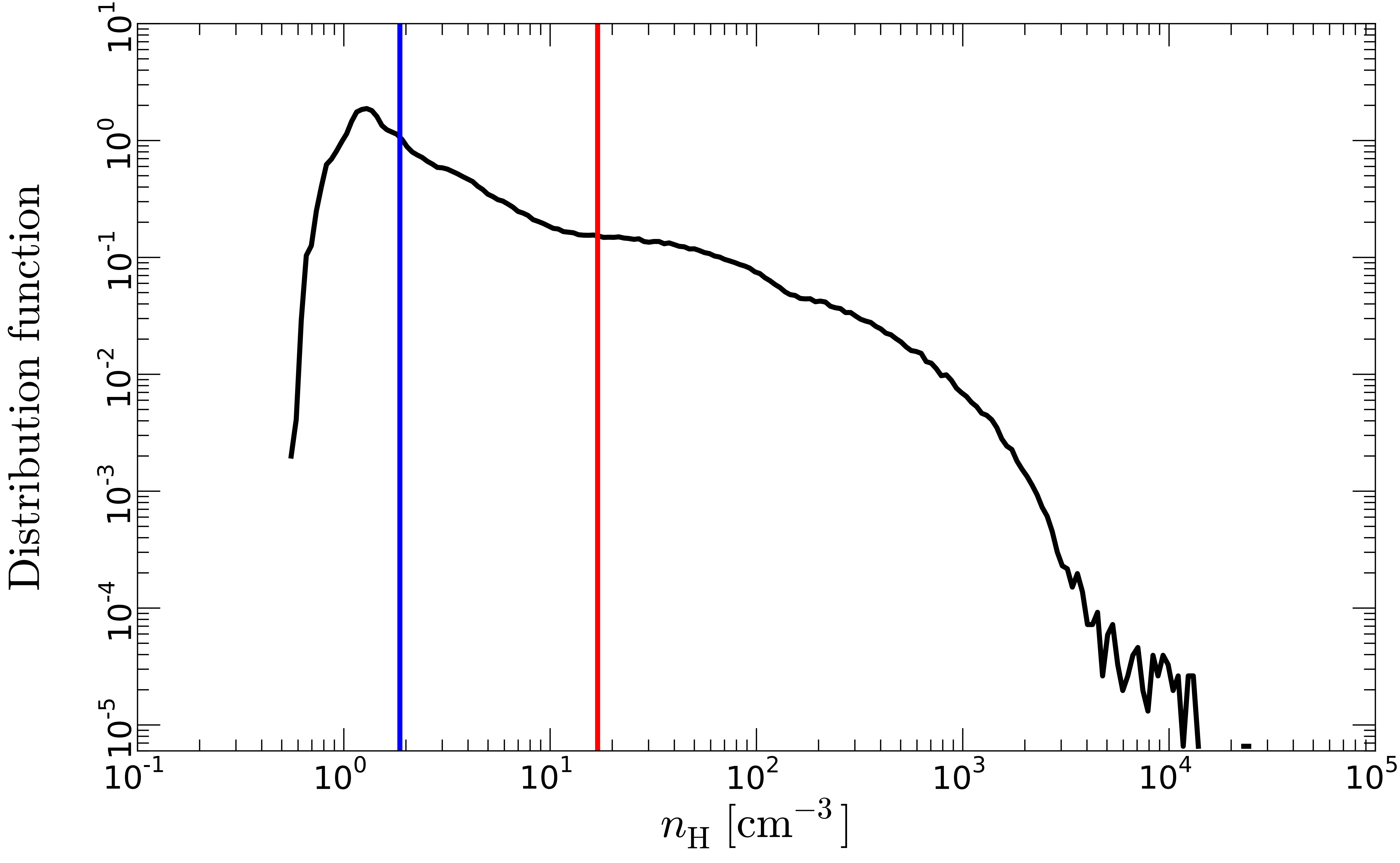

MHD simulation magnetic field PDF

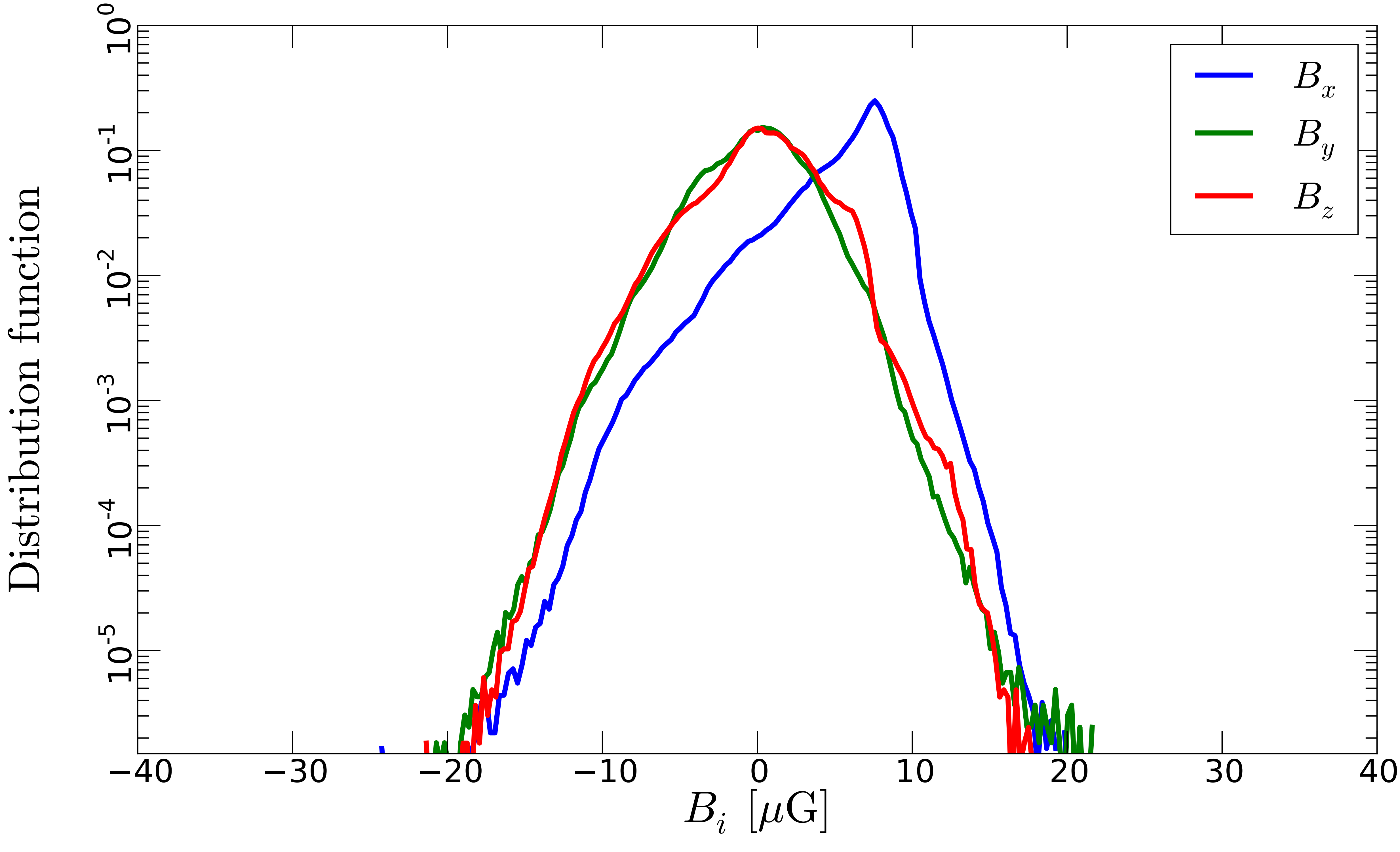

MHD simulation magnetic field power spectrum

« You have no power-law here ! »

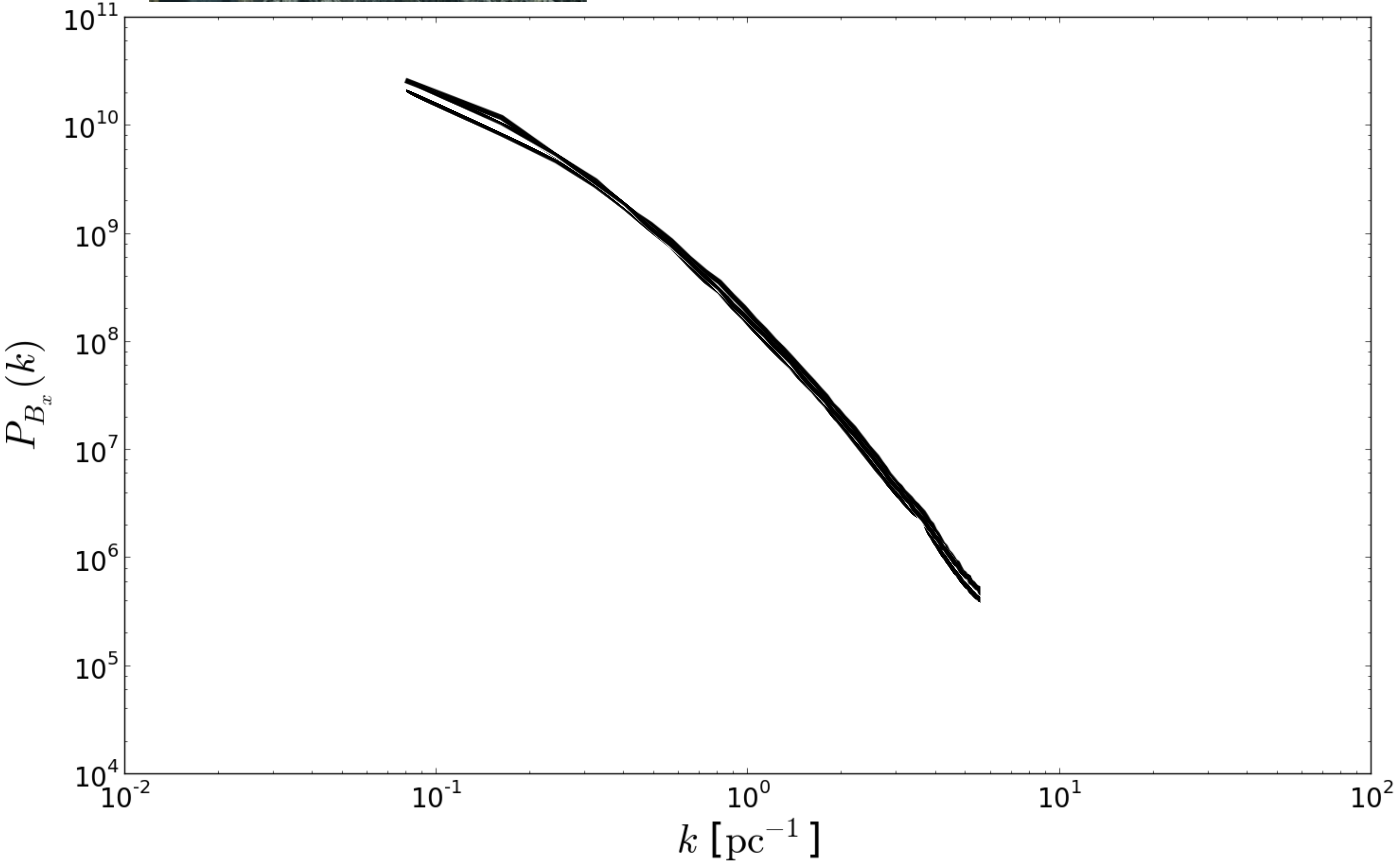

MHD simulation density power spectrum

« You have no power-law here ! »

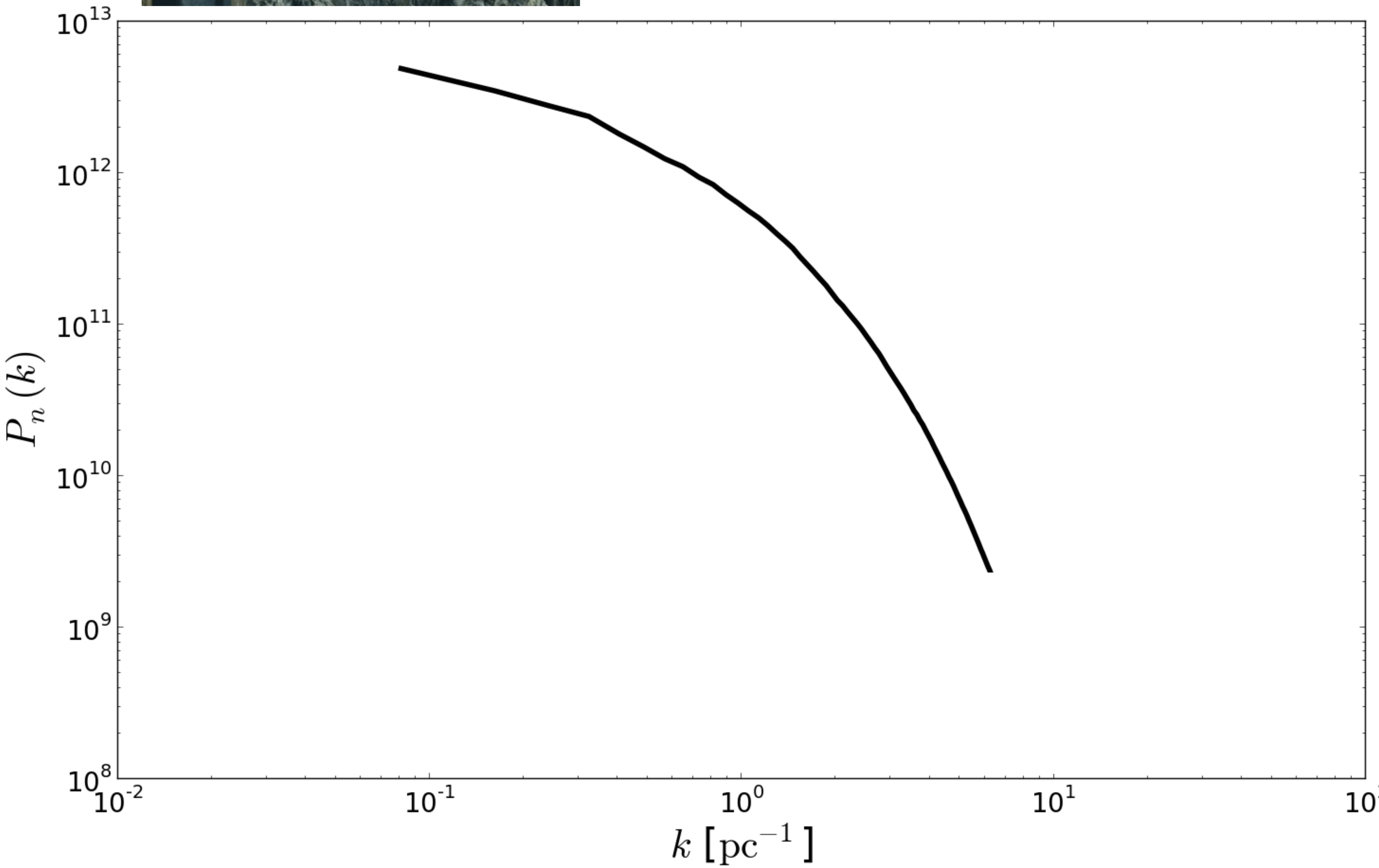

Properties of the dust density field

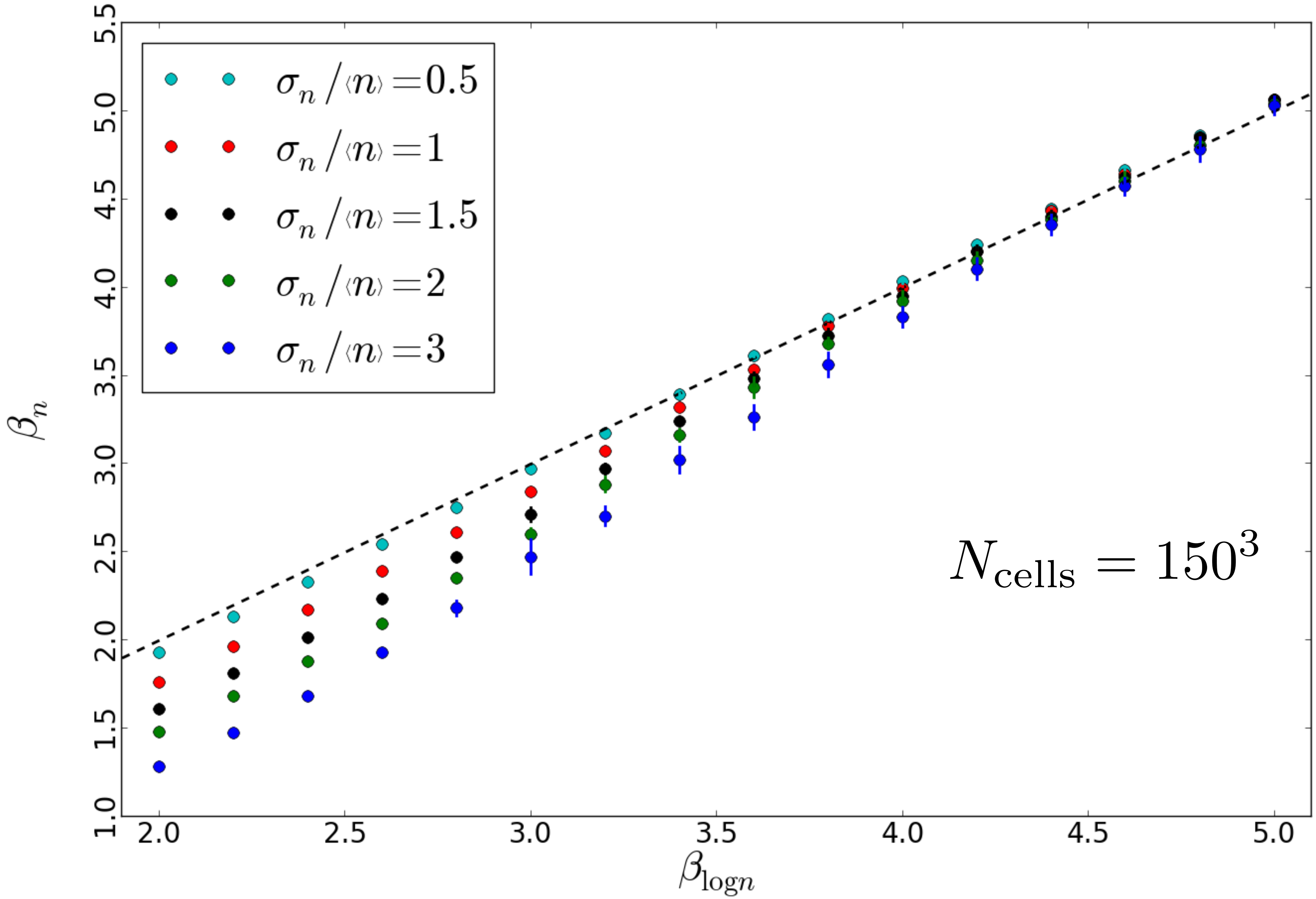

Density spectral index

Log-Density spectral index

Synthetic density field properties

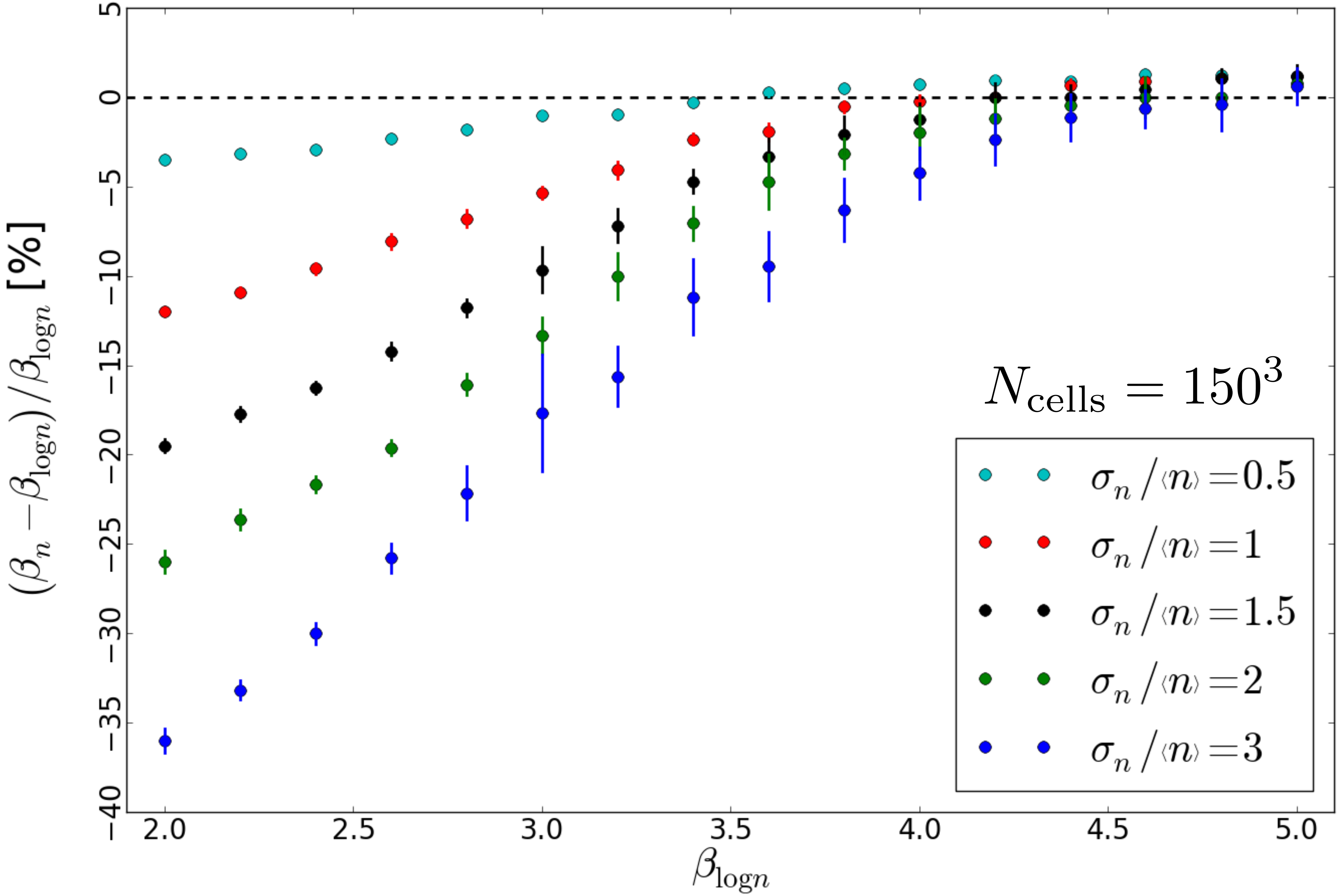

Relative difference

Log-Density spectral index

Synthetic density field properties

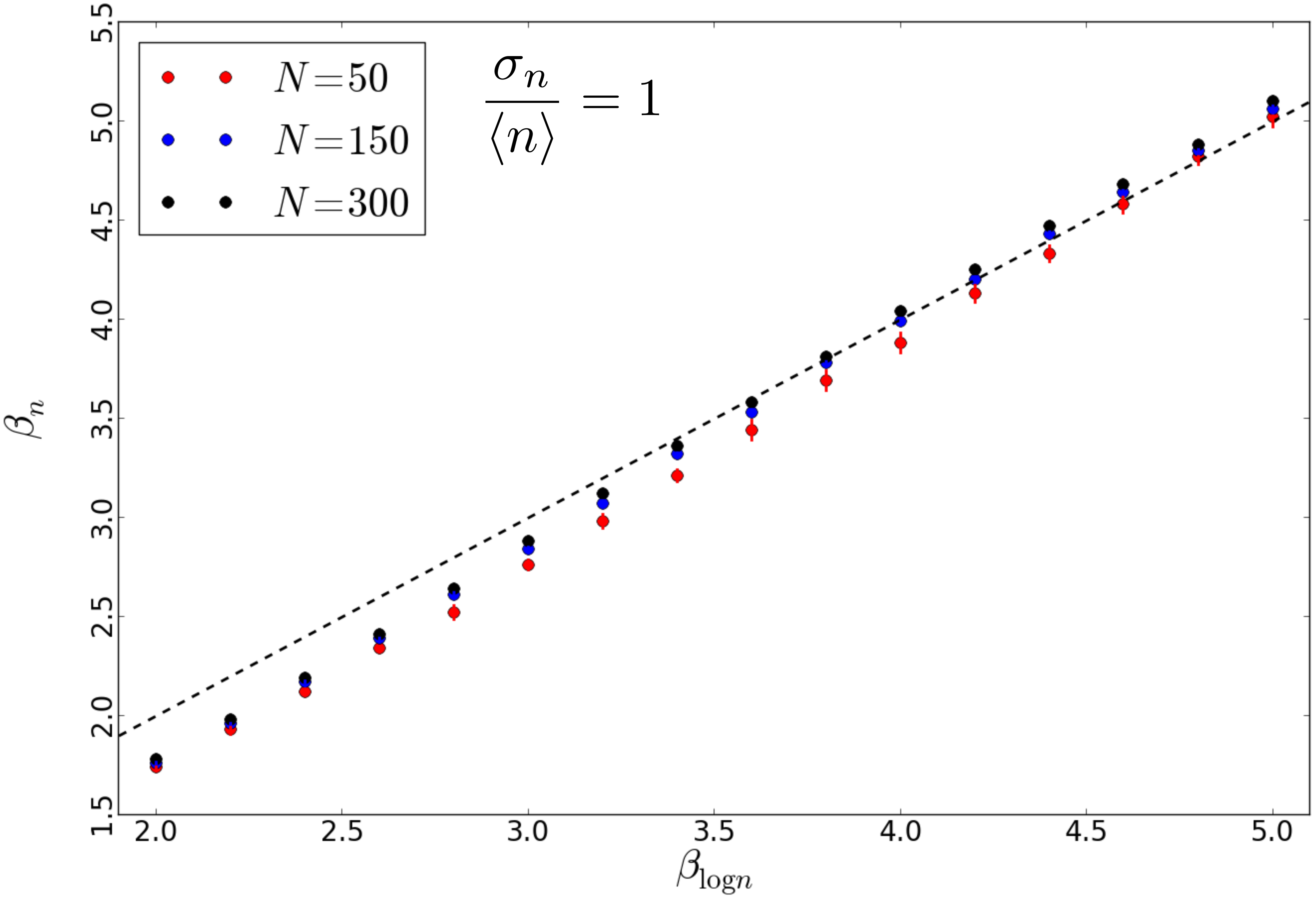

Density spectral index

Log-Density spectral index

Synthetic density field properties

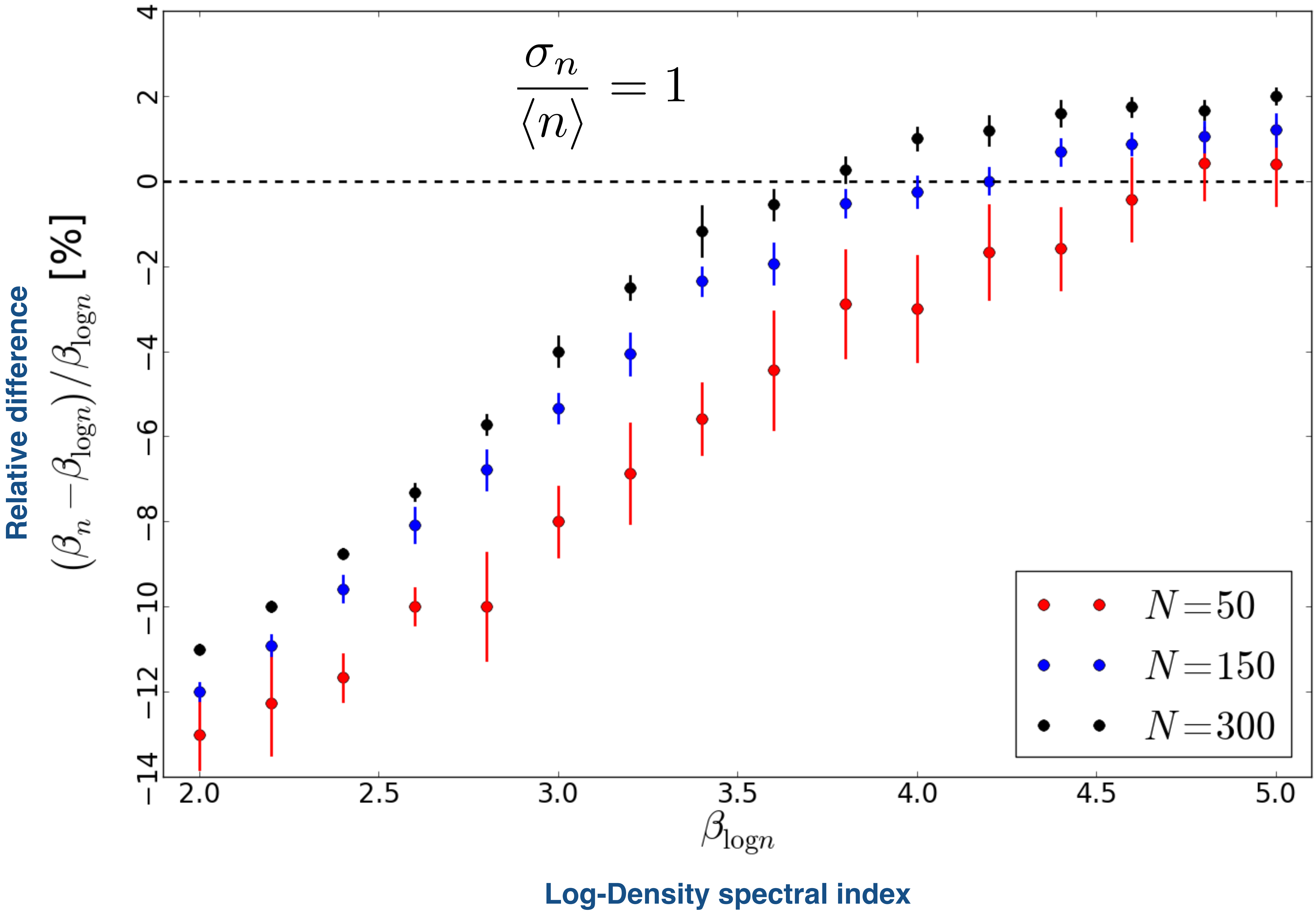

Synthetic magnetic field spectral index

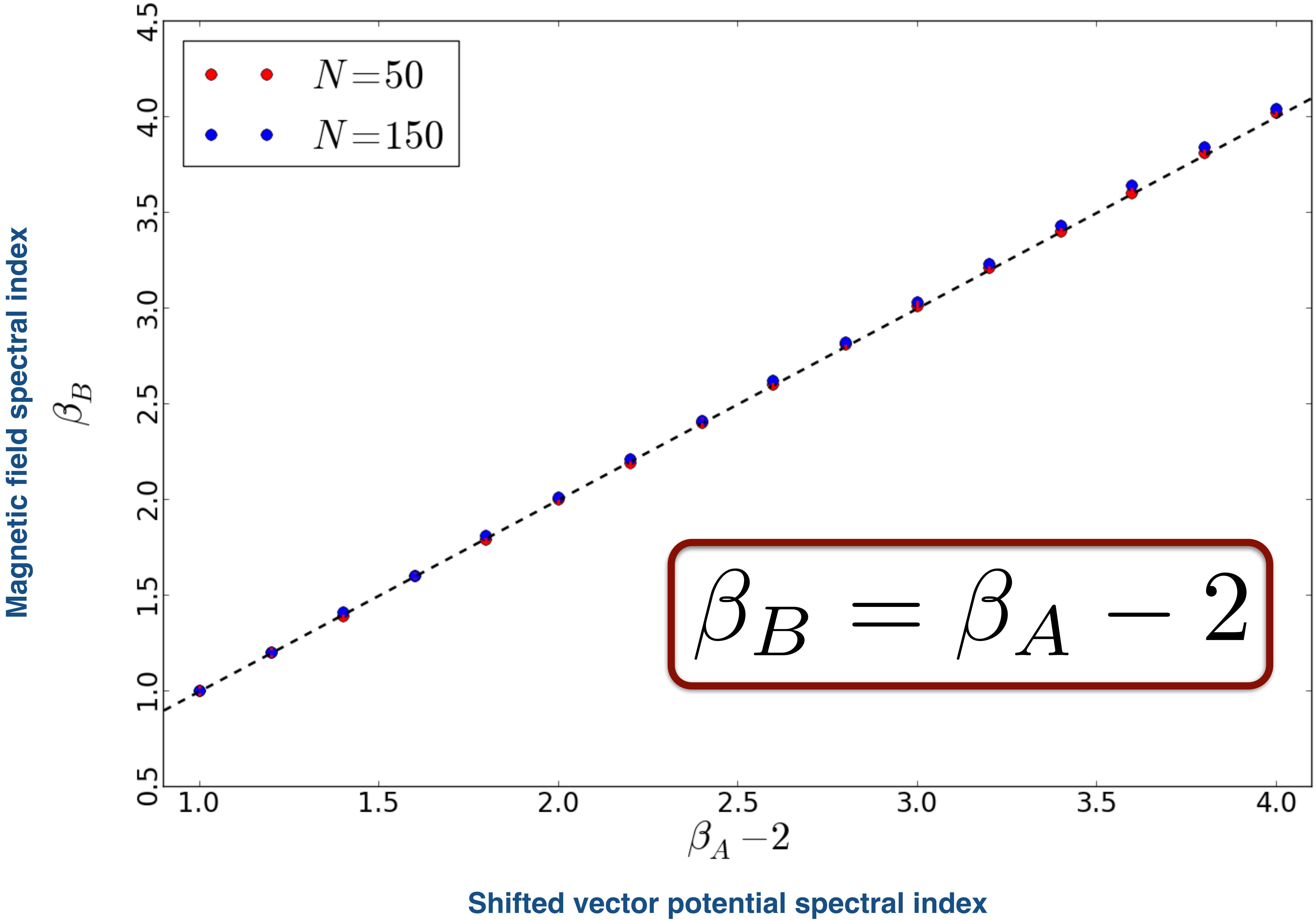

$$\beta_B = \beta_A - 2$$

fBm and exponentiated fBm

Slice of a 128x128x128 cube

Integration along one axis

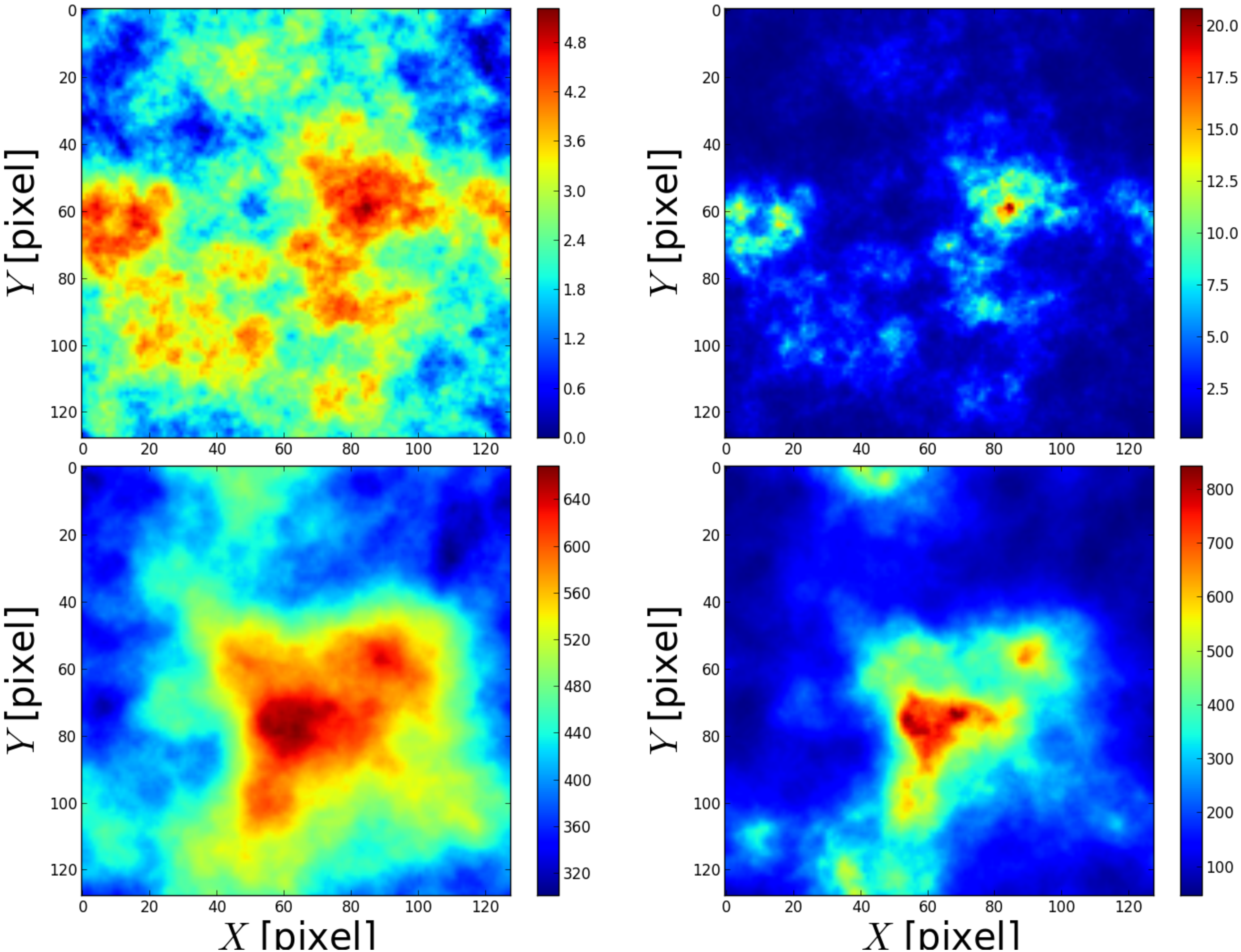

fBm

exponentiated fBm

Polarized thermal dust emission essentials

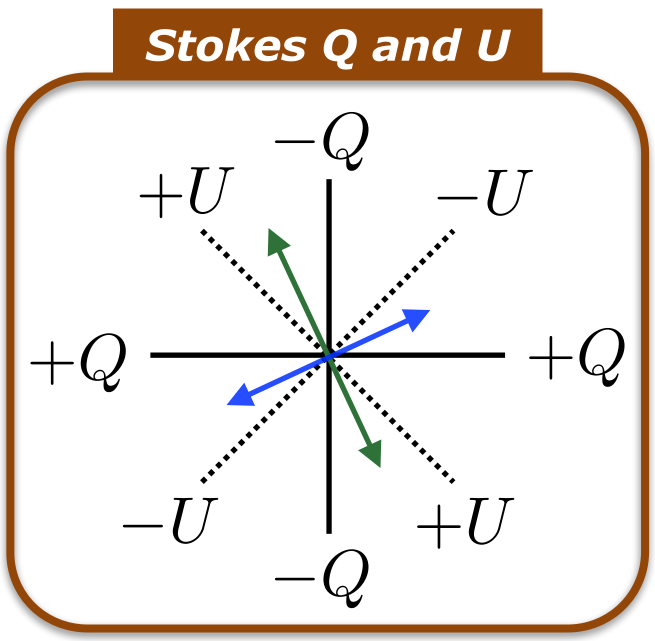

Polarization orientation
Magnetic field orientation

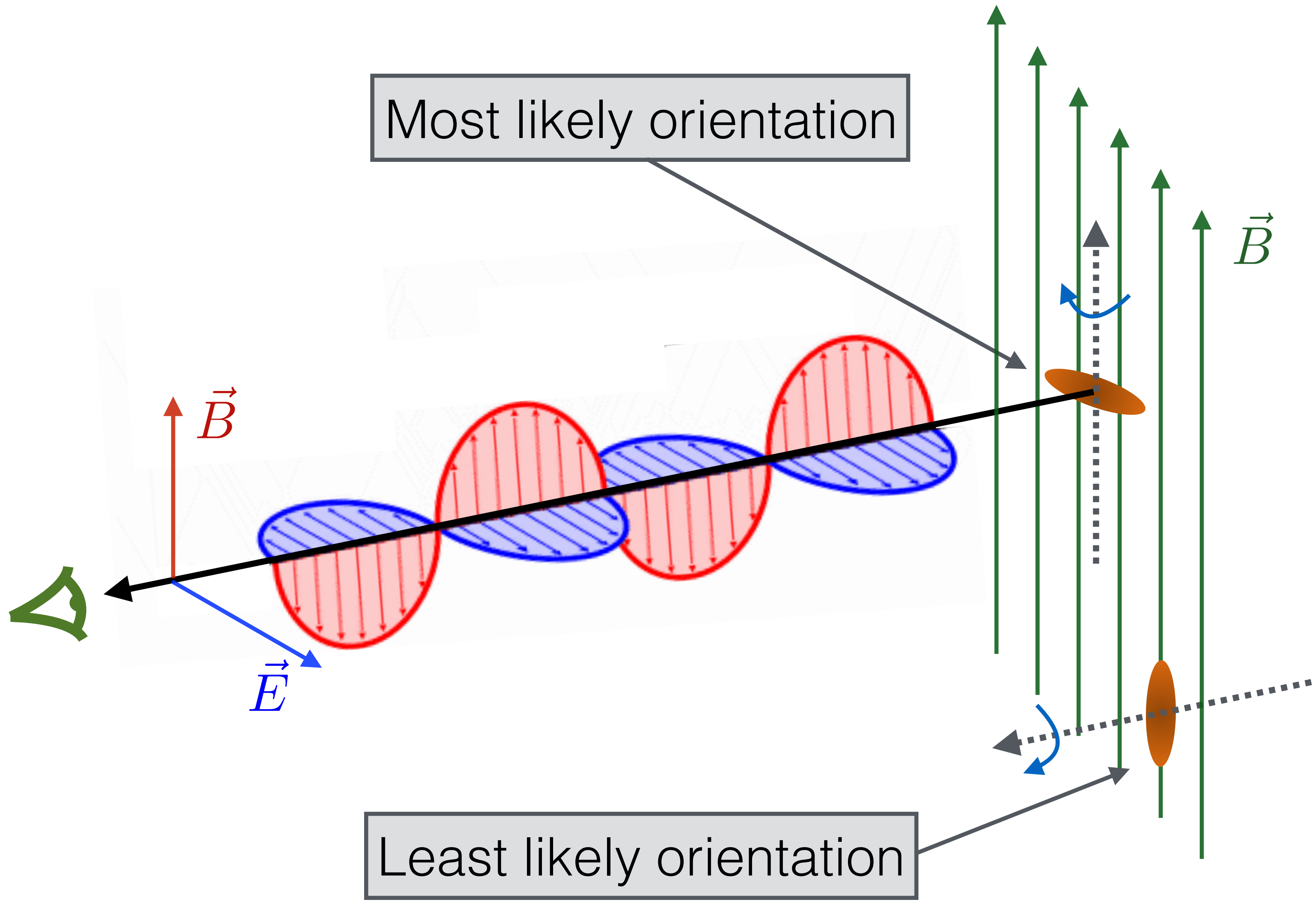

- Grains are aspherical, charged, rotating, and aligned preferentially perpendicularly to the local magnetic field
- Cross sections are proportional to the size, so grains emit more radiation parallel to their long axes
- Polarized thermal emission arises, with an orientation perpendicular to the local magnetic field

See Thiem Hoang's and François Boulanger's talks